EVALUATION OF SOLDER ALLOYS FOR BGA PACKAGE: A COMPARATIVE RELIABILITY STUDY USING ANSYS COMPUTATIONAL ANALYSIS

YASHVANTH MUTHEGOWDA

THESIS

Submitted in partial fulfillment of the requirements
for the degree of Master of Science in Mechanical Engineering at
The University of Texas at Arlington
MAY 2023

Arlington, Texas

Supervising Committee:

Dr. Dereje Agonafer, Supervising Professor
Dr. Abdolhossein Haji-Sheikh
Dr. Tushar Chauhan

Acknowledgements

I would like to thank Prof. Dereje Agonafer for his continuous support and guidance in my master's study and research. I would also like to thank him for his patience, motivation, and enthusiasm for this project. I am extremely glad to have been a part of the EMNSPC team. I would like to thank Dr. Abdolhossein Haji-Sheikh and Dr. Tushar Chauhan for being a part of my thesis committee.

A special thanks to Mr. Akshay Lakshminarayana, and Mr. Rabin Bhandari for their constant guidance and support. I had a great learning experience in the Reliability team working on different projects.

May 2023

Abstract

EVALUATION OF SOLDER ALLOYS FOR BGA PACKAGE: A COMPARATIVE RELIABILITY STUDY USING ANSYS COMPUTATIONAL ANALYSIS

Yashvanth Muthegowda, M.S.

The University of Texas at Arlington, 2023

Supervising Professor: Dereje Agonafer

Temperature cycling failure of solder joints in Ball Grid Array (BGA) packages has become a critical issue in electronic manufacturing. This thesis specifically characterizes three different lead-free solder alloys (Pure Indium, SAC-387, and SAC-Q) in BGA solder joints using two different printed circuit board (PCB) thicknesses (1mm and 0.7 mm). The analysis considers the non-uniform temperature distribution caused by the main heat source, the die, and the resulting deformation of the package due to the mismatch in the coefficient of thermal expansion (CTE) between components used in BGA. Finite element (FE) models are created in ANSYS mechanical package environment to predict stress distribution, plastic work, and the number of cycles to failure for different solder alloy compositions. Volume-averaged plastic work is calculated using an APDL script in ANSYS commands, utilizing stress and strain values from the FEA models. This research aims to evaluate the thermal reliability of solder alloys in BGA packages, as solder joint failures can result in device malfunctions or failures, leading to significant financial losses and reputational damage for electronic manufacturers. The findings of this study can contribute to the development of more reliable and durable electronic devices.

TABLE OF CONTENTS

Acknowledgments……..……III

Abstract……..……IV

List of Illustrations…….…..VII

Chapter 1 Introduction……...01

1.1 Electronic Packaging……...…01

1.2.Classification of Packages…….....04

1.3 Ball-Grid Array Package (BGA)……05

1.4 Classification of Solders…….06

1.5 Board-Level Reliability…….....07

1.6 Finite Element Method and Solder fatigue life prediction……...……..09

1.7 Thermal Cycling…….…..…...10

1.8 Objective…….……11

Chapter 2 Literature Review……..……13

Chapter 3: Computational Methodology…….....14

3.1 Introduction to Finite Element Method…….…….……14

3.2 FEA Problem-Solving Steps…….…..…...15

3.2.1 Geometry…….…….....……..16

3.2.2 Material Definition……...…….…….....16

3.2.3 Meshing the Model…….……...……16

3.2.4 Defining the Load and Boundary Condition…….……...…...…17

3.2.5 Setup and Solution……..…….....17

3.3 Geometrical Dimensions…….……...…....18

3.3.1 Package Geometry……..……18

3.3.2 Modelled Geometry……..….....20

3.3.3 Meshing……...20

3.3.4 Meshing Sensitivity…….……21

3.3.5 Material Properties……..22

3.3.6 Loading and Boundary Conditions……..……23

Chapter 4 Results…….....25
4.1Pure Indium……..…….……...25
4.1.1Stress Distribution…….…….……...25
4.1.1.1 Plastic Work (ΔW)…….…….....27
4.1.1.2 Number of Cycles to Failure (N_f)……..27
4.1.1.3 Conclusion…….…….....28
4.1.2 SAC 387 - 95.5%Sn - 3.8%Ag - 0.7%Cu …….....29
4.1.2.1 Stress Distribution…….....29
4.1.2.2 Plastic Work (ΔW)…….....30
4.1.2.3 Number of Cycles to Failure (N_f)……....31
4.1.2.4 Conclusion…….....32
4.1.3 SAC-Q - 92.7%Sn - 3.4%Ag - 0.5%Cu - 3.4%Bi……..33
4.1.3.1 Stress Distribution……..33
4.1.3.2 Plastic Work (ΔW)…….....35
4.1.3.3 Number of Cycles to Failure (N_f)…….....36
4.1.3.4 Conclusion…….…….....37
Chapter 5 Evaluation – Overall……...……..38
5.1 Stress Distribution……...……..38
5.1.1 Plastic Work (ΔW)…….....39
5.1.2 Number of Cycles to Failure (N_f)……...…...40
Chapter 6 Parametric Study……...…...41
6.1 Design of Experiments - Data and Comparison……..…….....41
Chapter 7 Conclusion……...…44
References…….……...……45

List of Illustrations

1. Figure 1-1 Packaging Level used in Electronics
2. Figure 1-2 Moore's Law
3. Figure 1-3 Classification of printed circuit boards
4. Figure 1-4 Ball-Grid Array Package Cross Section
5. Figure 1-4 -1 Ball-Grid Array Package Cross Section
6. Figure 1-5 Solder Joint
7. Figure 1- 6 View of BGA Solder Ball
8. Fig. 1 Problem-Solving Steps
9. Fig. 2 Package Geometry
10. Fig. 3 Components
11. Fig. 4 Modelled Geometry
12. Fig. 5 Meshing
13. Fig. 6 Meshing Sensitivity Analysis
14. Fig. 7 Solder Alloy – Anand's Viscoplastic
15. Fig. 8 Components Material Properties
16. Fig. 9 Temperature Cycling Plot
17. Fig. 10 Stress Distribution for 1mm
18. Fig. 11 Stress Distribution for 0.7mm
19. Fig. 12 Change in Plastic Work ΔW (MPa)
20. Fig. 13 No. of Cycles to failure
21. Fig. 14 Life cycles to failure (N_f) – Comparison
22. Fig. 15 Stress Distribution for 1mm

23. Fig. 16 Stress Distribution for 0.7mm

24. Fig. 17 Change in Plastic Work ΔW (MPa)

25. Fig. 18 No. of Cycles to failure

26. Fig. 19 Life cycles to failure (Nf) – Comparison

27. Fig. 20 Stress Distribution for 1mm

28. Fig. 21 Stress Distribution for 0.7mm

29. Fig. 21- 1 Change in Plastic Work ΔW (MPa)

30. Fig. 22 No. of Cycles to failure

31. Fig. 23 Life cycles to failure (N_f) – Comparison

32. Fig. 24 Stress Distribution – Comparison

33. Fig. 25 Plastic Work (ΔW)– Comparison

34. Fig. 26 No. of Cycles to failure

35. Fig. 27 Baseline PCB

36. Fig. 28 DP1 Results for 1mm

37. Fig. 29 Baseline vs Parametric for 1mm

38. Fig. 30 DP1 Results for 0.7mm

39. Fig. 31 Baseline vs Parametric for 0.7mm

40. Fig. 32 Design of Experiments

Chapter 1: Introduction

1.1 Electronic Packaging

Electronic packaging plays a crucial role in the modern world, enabling the development of various electronic devices that have become an integral part of our daily lives. From smartphones and laptops to smart appliances and medical devices, electronic packaging is essential for protecting, connecting, and powering electronic components, ensuring their reliable performance in a wide range of applications.

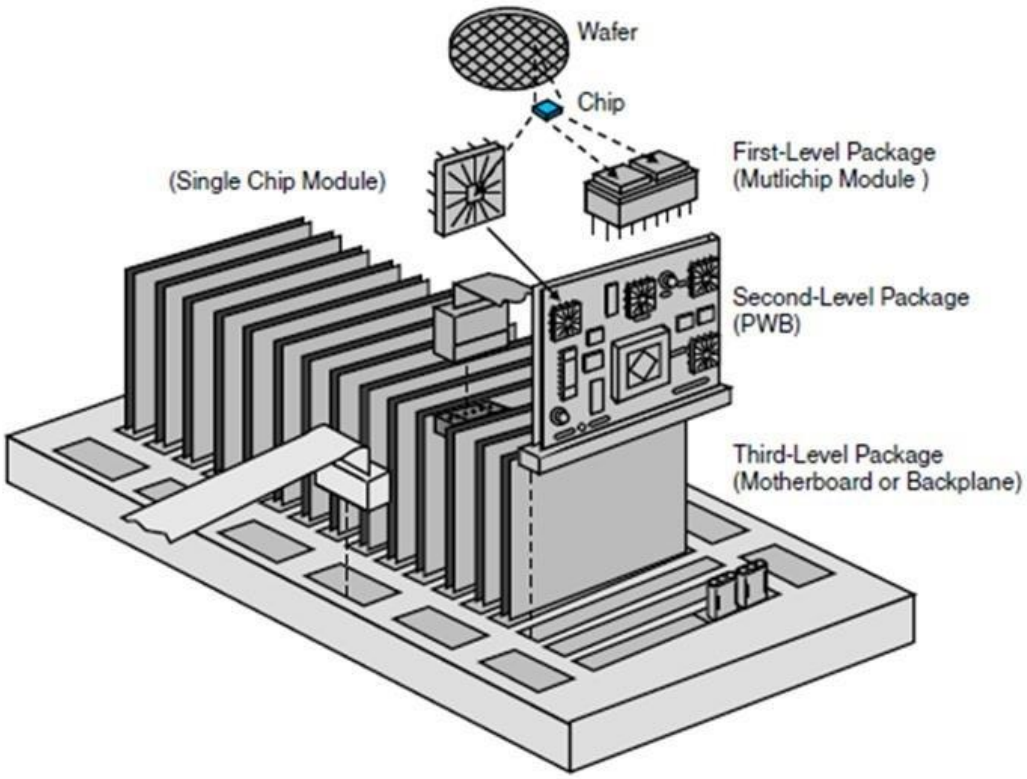

Figure 1-1 Packaging Level Used in Electronics [1]

Electronic packaging involves the interconnection and protection of electronic components, such as integrated circuit chips, displays, diodes, and power supplies, in a compact

and reliable manner. It encompasses various technologies and materials, including printed circuit boards (PCBs), chip-scale packages (CSPs), ball grid arrays (BGAs), and more. Electronic packaging serves as a bridge between the internal electronic components and the external world, providing electrical connectivity, thermal management, mechanical support, and environmental protection.

Knowing the viscoelastic behavior of the different components of electronic packages is important in order to perform accurate reliability assessment and design components such as PCBs that will remain dimensionally stable after the manufacturing process. [2]

The advancement of electronic packaging has been driven by the rapid progress of microelectronics, with the miniaturization of electronic components and the demand for higher performance, increased functionality, and lower cost. Electronic packages are required to meet stringent requirements for reliability, durability, and performance in various operating conditions, ranging from consumer electronics to aerospace and automotive applications.

Thermal conductive gap filler materials are used as thermal interface materials (TIMs) in electronic devices due their numerous advantages, such as higher thermal conductivity, ease of use, and conformity. [3]

According to Moore's law, "The number of transistors will double every 18 months". It is because of this law that Micro-processor industry has shown such exponential growth over the past few decades.

However, in recent years, there has been a decline in the rate of transistor scaling as we approach the physical limits of semiconductor manufacturing processes. This decline is due to various technological and economic challenges, such as increasing costs, power density issues,

and limitations in materials and manufacturing techniques, that make it increasingly difficult to sustain the exponential growth predicted by Moore's Law.

It is shown that sample preparation and characterization techniques have a considerable impact on the measurements, which results in different MEMS sensor performance predictions through computational modeling. [4]

As the demand for smaller, faster, and more efficient electronic devices continues to grow, there is a need for innovative solutions to overcome the limitations of traditional semiconductor technologies. This has led to extensive research and development efforts in exploring new materials, manufacturing processes, and packaging techniques to address the challenges associated with the declining trend of Moore's Law. One critical area of research in electronic packaging is the development of new solder alloys. [5]

Solder alloys play a vital role in electronic packaging, as they are used for interconnecting electronic components and providing reliable electrical and mechanical connections. With the miniaturization of electronic devices and the increasing complexity of packaging configurations, solder joints are subjected to various stresses, such as thermal cycling, mechanical vibrations, and power cycling, that can affect their reliability. The reliability of solder joints is crucial for ensuring the long-term performance and durability of electronic devices, as failures in solder joints can lead to device malfunctions, downtime, and costly repairs or replacements.

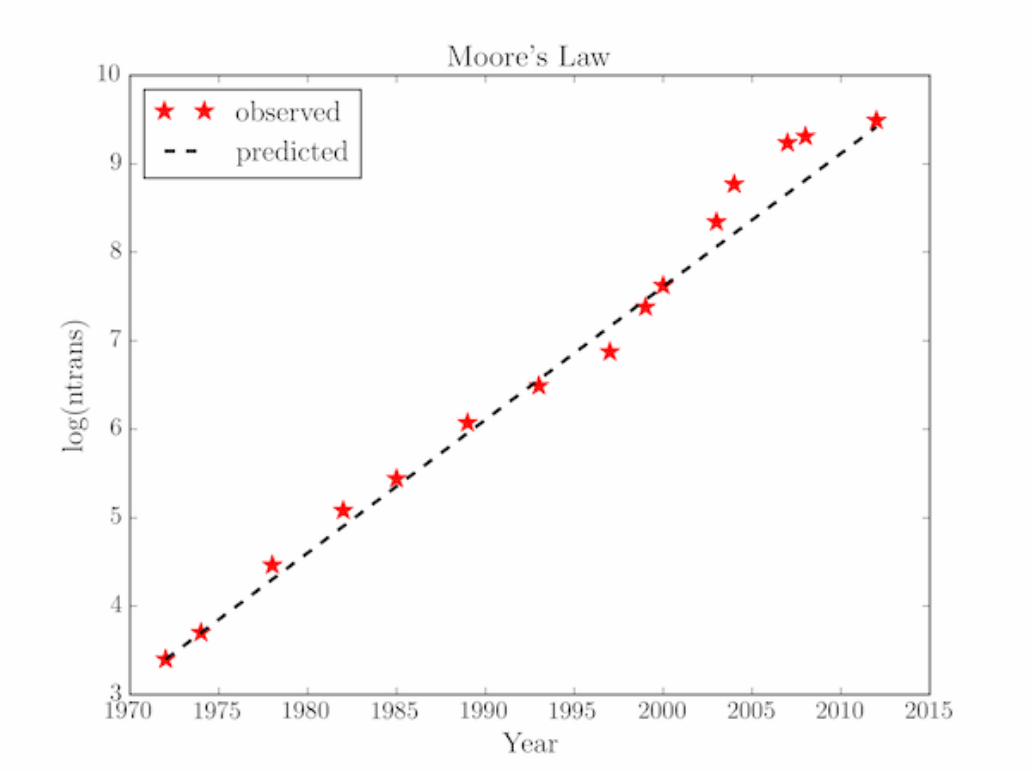

Figure 1-2 Moore's Law

1.2 Classification of Packages

PCBs (Printed Circuit Boards) can be classified based on various factors including material, wiring, rigidity, additives, structure, layer count, size, complexity, and manufacturing process. They can be single-layer, double-layer, or multi-layer, rigid, flexible, or rigid-flex. PCBs can vary in size, complexity, and intended application, and can be made of materials such as FR-4, polyimide, metal core, or ceramic. The manufacturing process can involve conventional through-hole technology, surface-mount technology (SMT), or mixed technology. PCBs are highly versatile and can be customized to meet specific requirements, making them an essential component in a wide range of electronic devices and systems.

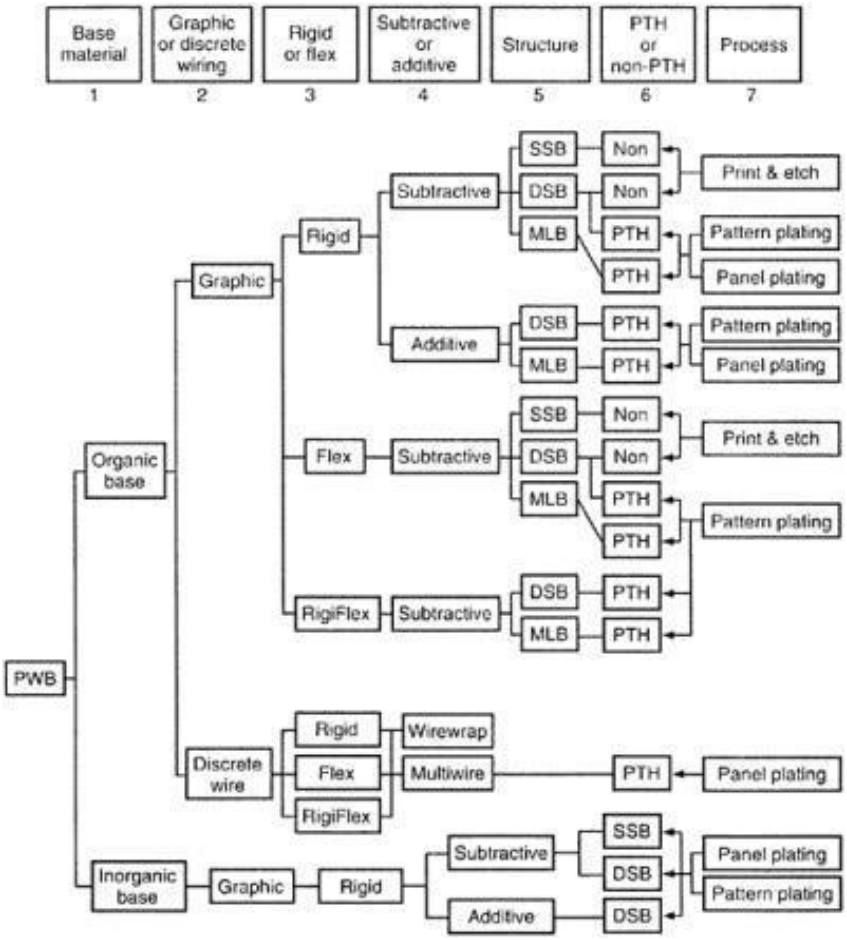

Figure 1-3 Classification of printed circuit boards

1.3 Ball-Grid Array Package (BGA)

Surface mount packages known as Ball Grid Arrays (BGAs) are frequently utilized for high-performance electronic components like processors and graphics cards. The BGA package is made up of a variety of little metal balls that are placed in a grid pattern on its underside.

The BGA package's high pin density is one of its main benefits. A BGA package can fit a lot of I/O (Input/Output) connections in a little amount of space since the metal balls are relatively small. This makes it possible to create electrical devices with smaller form factors that are more sophisticated and complex.

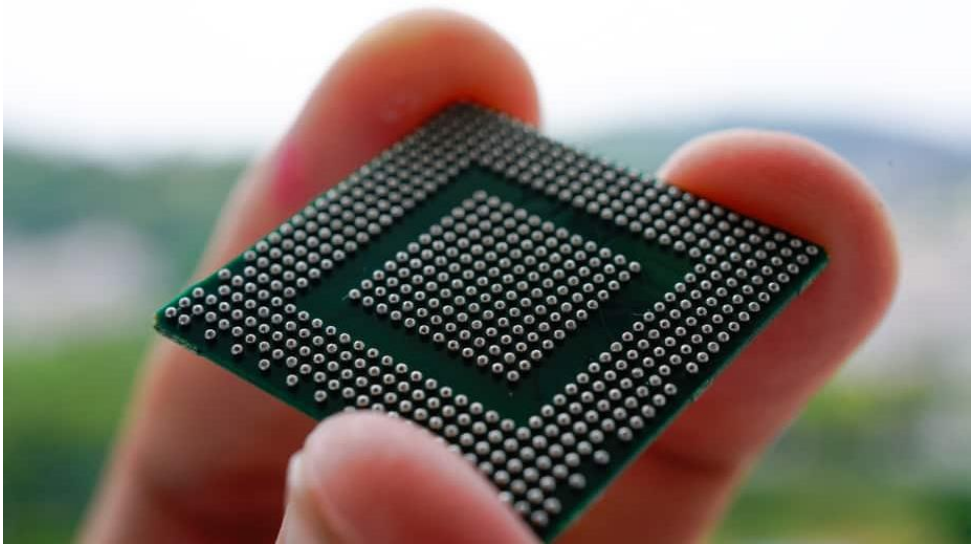

Figure 1-4 Ball-Grid Array Package Cross Section [5]

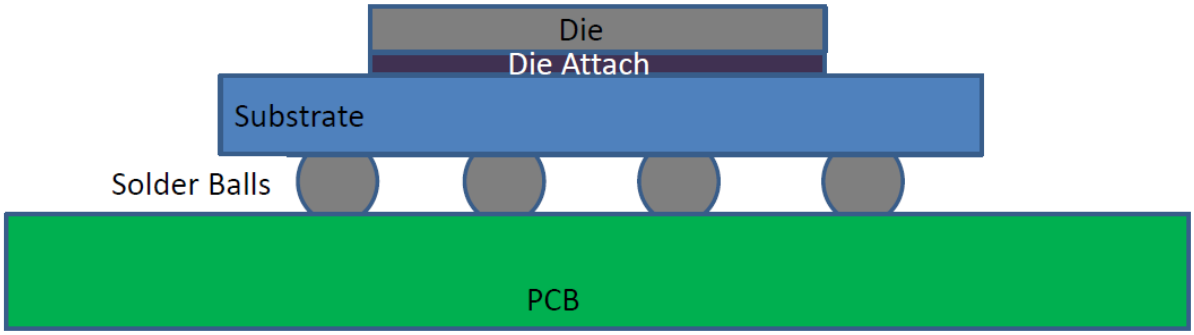

Figure 1- 4 Ball-Grid Array Package Cross Section

1.4 Classification of Solders

Electronic packaging, which involves joining or bonding electronic components to printed circuit boards (PCBs) or other substrates, plays a critical role in the manufacturing of electronic devices. Solder, a metal alloy with a low melting point, is the primary material used for this purpose. Soldering enables the creation of electrical connections and mechanical bonds between components and PCBs, allowing for the flow of electrical signals and power.

Solders are classified based on their composition, melting temperature, and intended application. Traditionally, lead-based solders, which contain lead as a major constituent, were widely used in electronic packaging. However, due to environmental concerns and regulations, lead-free solders have gained prominence as a more environmentally friendly alternative. Lead-free solder alloys, such as SAC387, SAC-Q, and Pure Indium, have been explored in this paper for better understanding. [6]

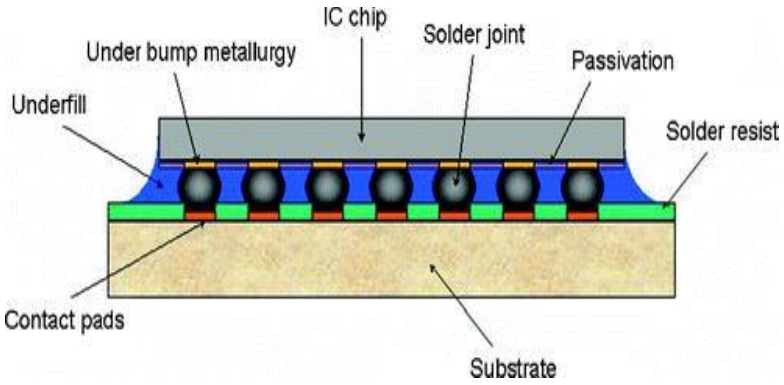

Figure 1-5 Solder Joint

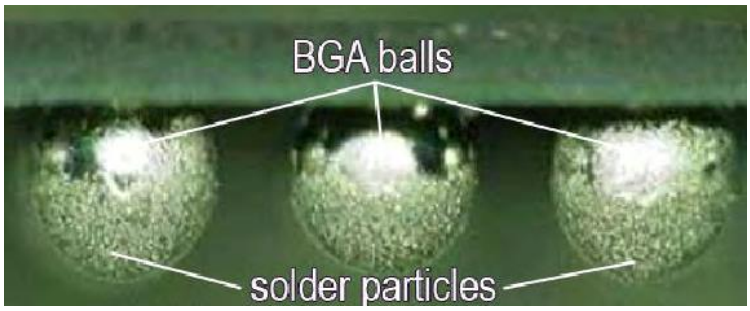

Figure 1- 6 View of BGA Solder Ball [7]

1.5 Board-Level Reliability

Reliability is an important aspect of electronic systems and components, including integrated circuits (ICs), as it refers to their ability to perform consistently and meet the required specifications over their expected lifespan. However, all products, including ICs, have a probability of failure, which can be estimated through reliability estimation techniques. [8]

Reliability estimation is typically based on subjecting the electronic system or component to various environmental stresses that simulate the working conditions it may experience during its operational life. These stresses help uncover any marginalities in materials or processes that could potentially lead to failures. While temperature changes are commonly considered as a stress factor, there are various other types of stresses that can affect reliability, such as environmental conditions, geometry, reversibility, and material properties.

The severity of stress levels can vary significantly depending on the specific application and environmental conditions. Different types of stresses that can impact electronic systems and components include mechanical stress from vibration or shock, thermal stress from temperature cycling or thermal aging, electrical stress from voltage or current variations, and environmental stress from moisture, chemicals, or radiation exposure. Understanding the different types of stresses and their impact on reliability is crucial in designing reliable electronic systems and components.

Few consortiums such as Joint Electronic Device Engineering Council (JEDEC) and Institute for Printed Circuits (IPC) have adapted, documented and standardized many of the reliability tests.

There are several key aspects of board level reliability that are commonly considered in electronic packaging:

1. **Solder Joint Reliability**: Solder joints, which are used to join electronic components to the PCB, play a critical role in the reliability of electronic products. The quality of solder joints, including their integrity, mechanical strength, and resistance to thermal cycling and mechanical stresses, directly affects the reliability of the PCB or the electronic system.

2. **Thermal Reliability**: Temperature changes during operation, such as temperature cycling or thermal aging, can cause stresses and strains on the PCB and its components, leading to potential failures. Thermal reliability involves designing the PCB and selecting materials that can withstand the expected temperature variations and thermal stresses during the product's operational life.

3. **Mechanical Reliability**: Mechanical stresses, such as vibration, shock, and bending, can impact the reliability of electronic products. Mechanical reliability involves designing the PCB and the electronic system to withstand these mechanical stresses without causing failures or degradation in performance.

4. **Environmental Reliability**: Environmental factors, such as humidity, moisture, chemicals, and radiation, can affect the reliability of electronic products.

5. **Electrical Reliability**: Electrical stresses, such as voltage or current variations, electrostatic discharge (ESD), and electromagnetic interference (EMI), can impact the reliability of electronic products. Electrical reliability involves designing the PCB and the electronic system to withstand these electrical stresses and prevent potential failures or degradation in performance. [10]

1.6 Finite Element Method and Solder fatigue life prediction

There are a lot of Finite-element based analysis that have been used to predict solder joint fatigue life like Coffin-Manson, Engel Maier, Darveaux, Blattau and Norris-Landzberg models. Out of these, Darveaux’s seems to be the most popular due to its easy implementation. Darveaux’s methodology links crack growth rate to inelastic work of solder. It is a strain energy-based approach, here the work term consists of time-independent creep and plasticity. This Inelastic

behavior is capture in ANSYS using Anand's constitutive model. The modelling methodology utilizes FEM to calculate the viscoplastic strain energy density accumulated per cycle during thermal cycling. The strain energy density is then used with crack growth values to calculate the number of cycles to initiate a crack, and the number of cycles for the crack to propagate across a solder joints diameter. Darveaux's methodology has presented in the successful analyses of various electronic assemblies from multiple industry sources. In many of these sources, reliability test data that validates the accuracy of Darveaux's methodology which is considered state of the art for this type of complex physical analysis. This energy-based model is used in this study to predict the solder joint life of the Solder. [11]

For example, temperature cycles can induce thermal as well as shear stresses in the solder joints. Shear stresses are induced by in plane thermal expansion due to CTE mismatch between component and the substrate. The external clamping forces and the internal thermomechanical forces causes the warpage of the substrate which induces out of plane tensile peeling forces [7].

Solder fatigue life prediction using FEM can be a valuable tool in the design and manufacturing of electronic products, as it allows engineers to optimize the solder joint design, materials selection, and operational conditions to ensure reliable performance and durability of electronic products.

1.7 Thermal Cycling

Thermal cycling, also known as accelerated thermal cycling (ATC), is a loading condition in which a device is repeatedly switched on and off, inducing thermal stresses in the system. This can lead

to fatigue failure of solder interconnects, which is a major factor affecting the reliability and lifespan of electronic packages.

To estimate the fatigue life of solder interconnects, accelerated thermal cycling is often used as a test method, where hundreds of parts are subjected to repeated thermal cycles to simulate the expected operational conditions over the device's lifespan. Numerical integration tools such as Finite Element Analysis (FEA) are commonly used for virtual qualification, aiming to reduce development time and expenses.

However, in practical conditions, the temperature distribution in the assembly during thermal cycling is non-uniform, as the die is typically the only source of heat generation. This results in differences in the coefficient of thermal expansion (CTE) between components, leading to deformation of the package. This deformation may differ from that observed during accelerated thermal cycling, where uniform temperature conditions are assumed.

It is important to consider these practical conditions and the non-uniform temperature distribution during thermal cycling when using numerical tools like FEA for solder fatigue life prediction. Validating the predictions with experimental data and accounting for other factors such as manufacturing variability, environmental conditions, and product usage can help ensure accurate and reliable predictions of solder fatigue life in real-world applications.

1.8 Objective

The objective of this thesis is to investigate the thermal reliability of three different lead-free solder alloys in BGA packaging under temperature cycling (-40◦C to - 125 ◦C) until failure. The study aims to compare the performance of Pure Indium, SAC-387, and SAC-Q solder alloys on two different printed circuit board (PCB) thicknesses, 1mm and 0.7mm.

In this study, Finite Element (FE) models were developed for each of the solder alloy compositions. These models were used to predict the stress distribution, plastic work, and the number of cycles to failure for each of the solder alloys. The volume-averaged plastic work was also calculated using an APDL script in ANSYS commands, which allowed us to determine the amount of plastic deformation that occurs during the thermal cycling tests.

The results of this research provide valuable insights into the thermal reliability of the different solder alloys and their suitability for various electronic applications. By comparing the performance of the solder alloys on different PCB thicknesses, It is able to determine the effect of PCB thickness on the thermal reliability of the solder joints.

The findings of this study can contribute to the development of more reliable and durable electronic devices, which can have significant implications for various industries, including aerospace, automotive, and consumer electronics. By understanding the mechanical behavior and failure modes of these materials under thermal cycling, It is possible to improve the design and reliability of electronic devices that use these solder alloys.

Chapter 2 Literature Review

Pavan Rajmane [8] explored the issue of failure analysis and reliability concerns in electronic packaging. To obtain more accurate fatigue life predictions, it is necessary to consider all the affecting loads on electronic devices. It focused on the power cycling loading condition, which occurs when an electronic device is turned off and then turned on multiple times. He studied wafer-level chip scale package (WLCSP), which is a package technology that involves creating an array pattern of solder interconnects on a die at the wafer level. Since the die is the heat source, it causes nonuniform temperature distribution, resulting in thermal stresses due to the mismatch in the coefficient of thermal expansion (CTE) between the components used in WLCSP. finite element analysis (FEA) to assess the solder ball reliability of WLCSP under two different loads. They also cross-sectioned the printed circuit board (PCB) and observed that the life of any assembly also depends on the copper content.

Tong Yan Tee et al. [10] studied the board level solder joint reliability for both QFN and enhanced design of Power QFN under thermal cycling. They created a thorough solder joint fatigue model with the ability to forecast life with an error rate of just 34%. To improve the solder joint reliability of QFN, the researchers conducted a thorough design analysis to look at the effects of important factors on fatigue life. They recommended using a smaller package type, more center pad soldering, smaller die size, thinner die, bigger die pad size, thinner board, longer lead length/width, smaller pitch, higher solder standoff, solder with fillet, higher mold compound CTE, and a smaller temperature range of thermal cycling test. [13]

Chapter 3 Computational Methodology

3.1 Introduction to Finite Element Method

The Finite Element Method is a computational technique used to obtain approximate solution to boundary value problem in engineering. FEM is virtually used in almost every industry that can be imagined. Common application of FEA applications are mentioned here.

- Aerospace/Mechanical/Civil/Automobile Engineering
- Structural Analysis (Static/Dynamic/Linear/Non-Linear)
- Thermal/Fluid Flow
- Nuclear Engineering

There are three major ways to study the mechanical reliability of immersion cooling: experimental, analytical, and numerical. The experimental analysis is the most expensive among all three, and the problem at hand is too complex to study analytically. The numerical method proves itself as the cost- and time-effective approach, and as such, the finite element method is a popular and widely adopted numerical method. [8]

FEA is the computational technique which helps in reaching the satisfactory results with all the complex conditions that can't be solved through analytical procedure. There are wide range of sophisticated commercial code available which helps in reaching the approximately close solution in 1D, 2D and 3D. In this FEA method, the whole continuum is divided into a finite numbers of small elements of geometrically simple shape. These elements are made up of numbers of nodes. Displacement of these nodes is unknown and to find it, polynomial interpolation function

is used. External force is replaced by an equivalent system of forces applied at each node. By assembling the mentioned governing equation, results for the entire structure can be obtained.

$$\{F\} = [K]\{u\}$$

Where, {F} = Nodal load/force vector →[K] = Global stiffness matrix

{u} = Nodal displacement

3.2 FEA Problem Solving Steps

These five steps need to be carefully followed to reach satisfactory solution to FEA problem:

1) Geometry and Material definition

2) Defining Connection between bodies

3) Meshing the model

4) Defining load and boundary condition

5) Understanding and verifying the results

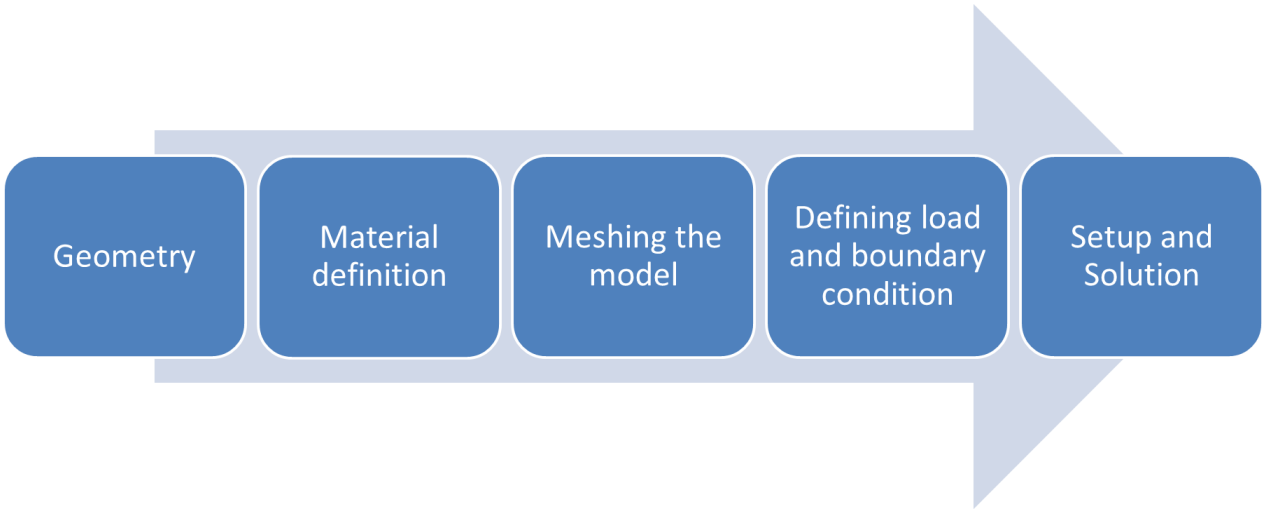

Fig. 1- 7 Problem-Solving Steps

3.2.1 Geometry

Prior to analysis, geometric nonlinearity must be taken into account. There are primarily two types of nonlinearity here.

1) Large deflection and rotation: If the structure's overall deformation is significant relative to its smallest dimension or rotates to the point where its dimensions, location, or loading direction considerably change, an analysis of large deflection and rotation is required. The significant rotation and deflection are due to a fishing rod.
2) Stress Stiffening: When stress is applied in one direction, the stiffness in the other direction is affected. Stress stiffening can be seen in cables, membranes, and other spinning structures. [12]

3.2.2 Material Definition

The correctness of the solution is impacted by material nonlinearity, which is another crucial component of FE analysis. Linear materials are a good approximation if they exhibit a linear stress-strain curve up to a proportionate limit or if they are loaded in a way that prevents stress levels higher than yield values anywhere in the body. Following consideration of the geometry and material characteristics, contacts between various bodies, such as those that are rigid, frictional, bonded, etc., must be taken into account.

3.2.3 Meshing the Model

A large mesh count (number of elements) offers a better approximation of the answer. There is a potential that in some situations, having too many factors causes the round off error to grow. It is crucial that the mesh is either fine or coarse in the proper area, and the answer to that question depends entirely on the physical system under consideration. Mesh sensitivity analysis is

sometimes taken into account to balance computation time with solution accuracy. The first round of analysis uses a particular amount of elements, while the second round uses twice as many.

3.2.4 Defining the Load and Boundary Condition

A crucial step in effectively replicating a system's behavior under various operating settings is establishing the load and boundary conditions. Any external force, pressure, or temperature acting on the structure under study is referred to as the load. This could involve thermal loads like heating or cooling as well as mechanical loads like tension, compression, or bending.

On the other hand, boundary conditions relate to the restrictions or limits placed on the system's behavior at particular places or regions. These may include immovable supports or restrictions, as well as set temperature or displacement requirements.

The FEA approach separates the continuum into a finite number of small, geometrically straightforward elements, each formed of a collection of nodes, after the load and boundary conditions have been established. By substituting analogous systems of forces applied to each node, the external forces acting on the structure are substituted to estimate the displacement of these nodes using polynomial interpolation functions. The results for the complete structure are then obtained by assembling the governing equations. The outcome can be used to examine the structural integrity of the system, improve its design, and gauge how well it performs under various operating scenarios.

3.2.5 Setup and Solution

The FEA model is solved using a computer program that employs numerical methods to determine the solution after the geometry, material properties, load, and boundary conditions have been established. The computer program breaks the model up into smaller components, computing

the solutions for each component using the governing equations. A comprehensive solution for the complete model is then created from the component solutions. It is necessary to solve a system of linear equations for this process, which can be done in a number of ways, including directly and iteratively.

The process of setting up and solving an FEA model is iterative, with the model and solution refined as needed to achieve an accurate and reliable result.

3.3 Geometrical Dimensions

3.3.1 Package Geometry

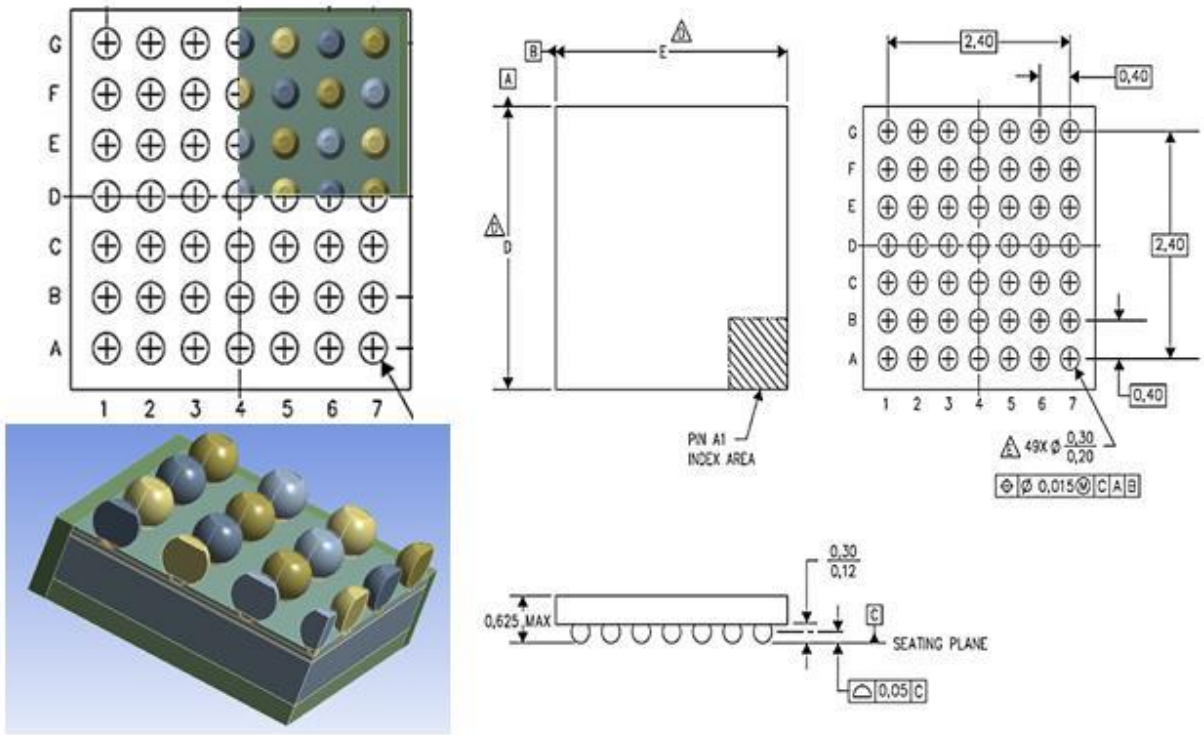

Fig. 2 Package Geometry [12]

Component	Dimensions (mm)
Package	2.8 x 2.8 x 0.43
Die	4.315 x 3.245 x 0.19
PI Layer	2.8 x 2.8 x .02
Die Attach	4.15 x 4.15 x 0.01
UBM	.07 x 0.03
Pitch	0.4
PCB	24 x 24 x 1.00 24 x 24 x 0.70

Fig. 3 Package Geometry [12]

3.3.2 Modelled Geometry

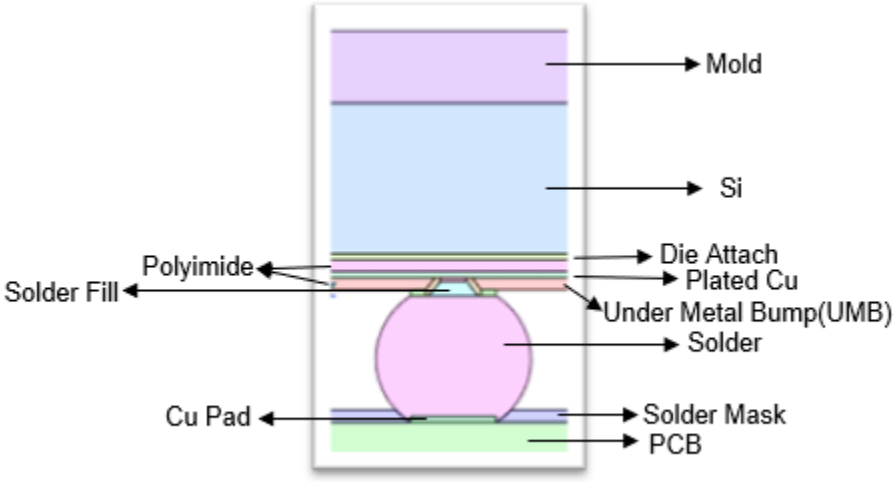

Fig. 4 Modelled Geometry

3.3.3 Meshing

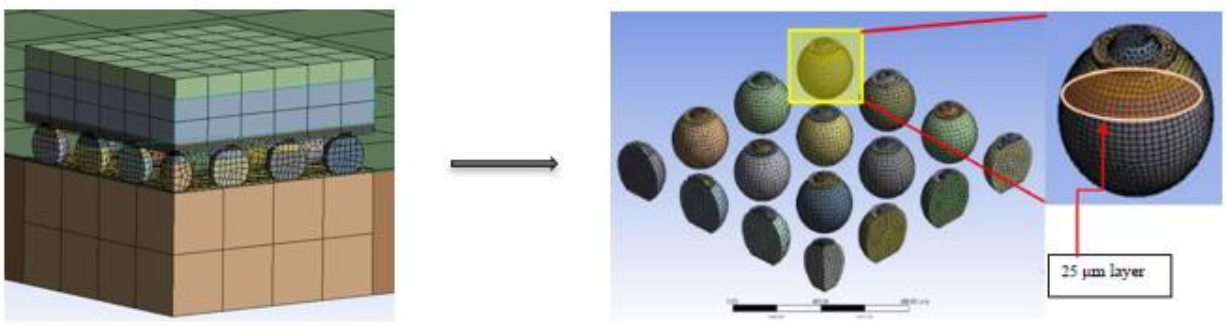

Fig. 5 Meshing

The quarter geometry has been adopted for simulation due to its ability to reduce computational time. The mesh sizes used in the simulation are assumed to be medium, with edge sizing applied to thin sections and body sizing applied to solder balls. To achieve the meshing, the hex-dominant method has been employed. To determine the life cycles to failure of both the boards, a 25µm layer, starting at the interface of the solder and the Under-Bump Metal (UBM), has been sliced inside the solder ball. [17]

3.3.4 Meshing Sensitivity

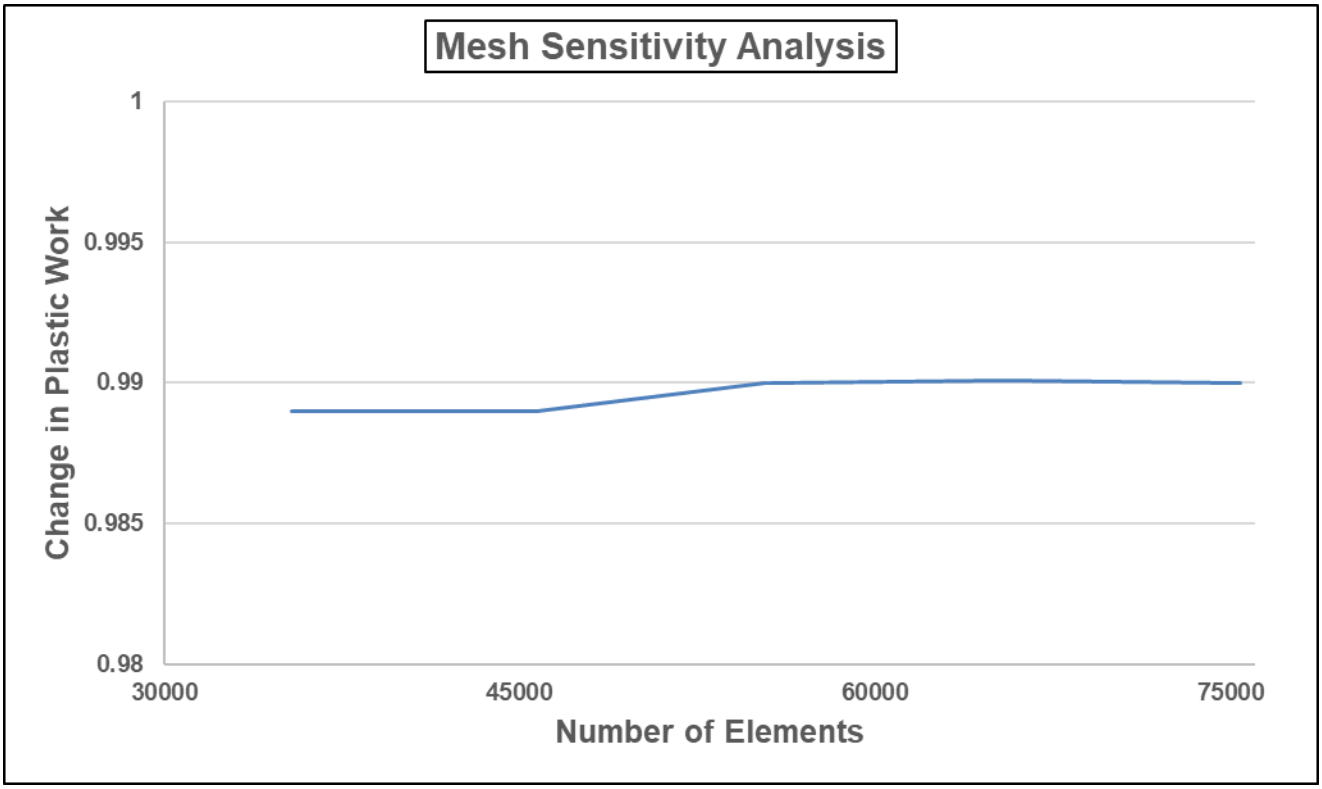

Fig. 6 Meshing Sensitivity Analysis

For the accurate determination of simulation results, it is crucial to ensure that the model is grid independent. [18] Hence, a mesh sensitivity analysis is conducted to validate the model's accuracy. In this analysis, mesh sizes are considered medium, as the observable variance was less than 2%, which indicates that the results are not significantly affected by the mesh size. [19] This approach not only saves computational time but also ensures that the simulation results are obtained within a reasonable timeframe.

3.3.5 Material Properties

As mentioned in the assumptions, Solder is modeled as rate dependent viscoplastic material which uses Anand's viscoplastic model. [20] It takes both creep and plastic deformation into consideration to represent secondary creep of the solder. [21] Anand's viscoplastic constitutive law best describes the inelastic behavior of lead-free solder. Anand's law consists of nine material constants A, Q, ξ, m, n, hu, a, s_u, ŝ.

Constant	Name	Unit
so	Initial Deformation Resistance	MPa
Q\R	Activation energy/Universal gas constant	1/K
A	Pre-exponential factor	1/sec
€	Multiplier of stress	Dimensionless
m	Strain rate sensitivity	Dimensionless
ho	Hardening constant	MPa
s	Coefficient of Deformation/Resistance Saturation	MPa

Fig. 7 Solder Alloy – Anand's Viscoplastic

In this study, all materials, except for the Solder alloy and PCB, are modeled as linear elastic. The PCB is modeled as linear orthotropic, which accounts for the anisotropic properties of the material. [22] On the other hand, the Solder alloy is modeled as viscoplastic using Anand's constants. This approach is suitable for modeling the time-dependent behavior of materials that exhibit viscoplasticity, such as solder alloys. [23]The use of Anand's constants enables the model to account for the material's rate-dependent behavior and accurately predict the deformation and failure of the solder alloy. By using a combination of linear

elastic and viscoplastic models, this study aims to provide a comprehensive understanding of the mechanical behavior of the materials under different loading conditions.

Material	Property						
	E	CTE(ppm/C)			v		
	(GPa)	X	Y	Z	xy	yz	xz
PCB (0.7mm)	30	18.3	16.7	30.2	0.11	0.39	0.39
PCB (1mm)	25	15.7	15.7	40.4	0.11	0.39	0.39
Die	131		3			0.28	
RDL	130		16.8			0.34	
Polyimide	1.2		52			0.25	
Mold	24		20			0.3	
Cu	110		17			0.34	
Solder Mask	4		30			0.4	

Fig. 8 Components Material Properties

3.3.6 Loading and Boundary Conditions

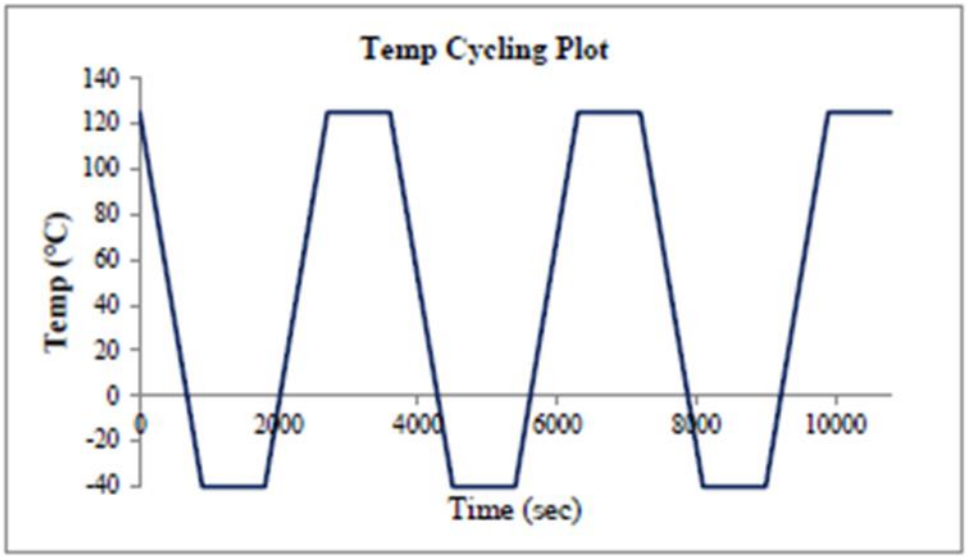

Fig. 9 Temperature Cycling Plot [12]

[13]The loading conditions for this study involve thermal cycling, where the temperature is cycled between -40°C to 125°C. To ensure accuracy, three cycles are used, each lasting 60 minutes with a ramp time of 15 minutes and a dwell time of 15 minutes. [25] The stress-free temperature of all bodies in the model is set to 125°C, and symmetric boundary conditions are applied to the two symmetric faces. Additionally, the center node of the full model is fixed to maintain stability during the simulation. [26]By using these loading conditions, this study aims to investigate the thermal behavior of the materials under cyclic loading and determine their ability to withstand such conditions. The results of this study will provide insight into the mechanical behavior of the materials under thermal cycling and aid in the development of more durable and reliable components. [27]

Chapter 4 Results

4.1 Pure Indium

4.1.1Stress Distribution

1mm PCB

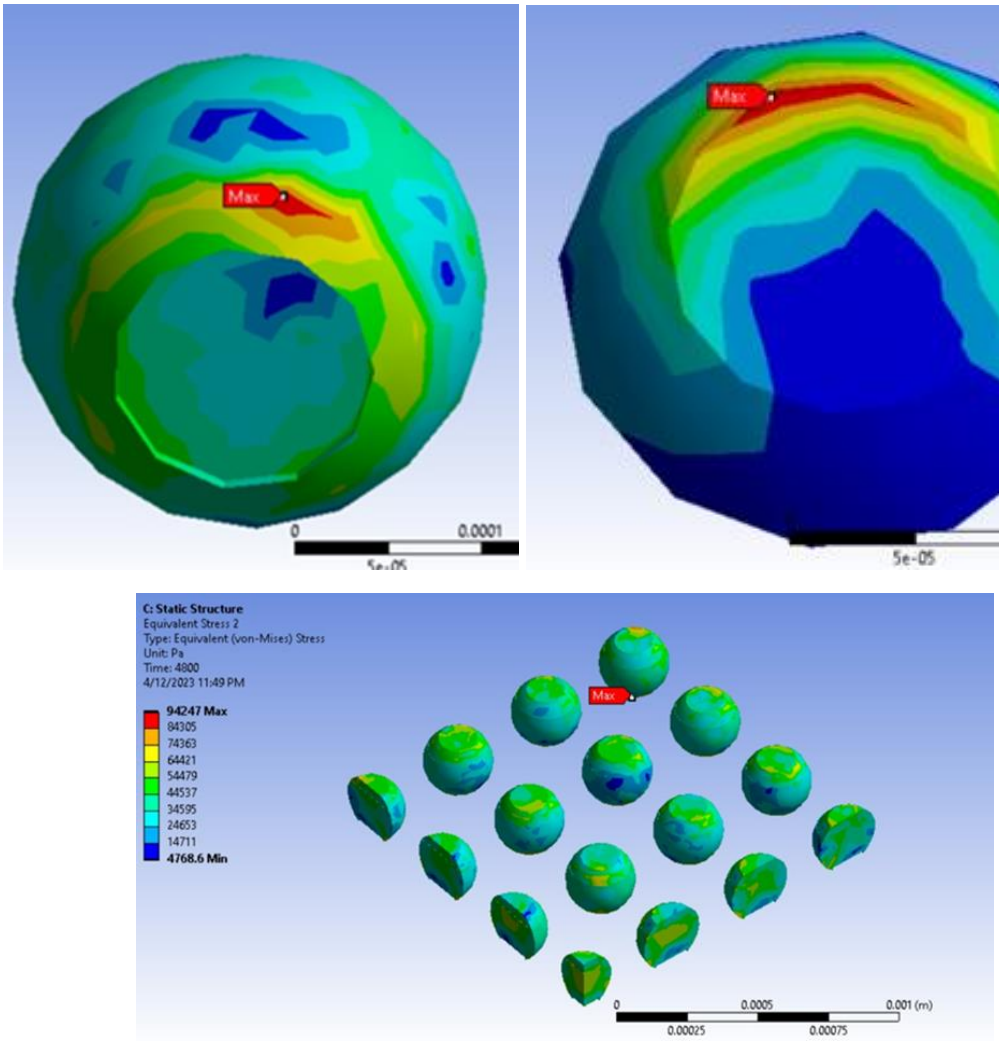

Fig. 10 Stress Distribution for 1mm

0.7mm PCB

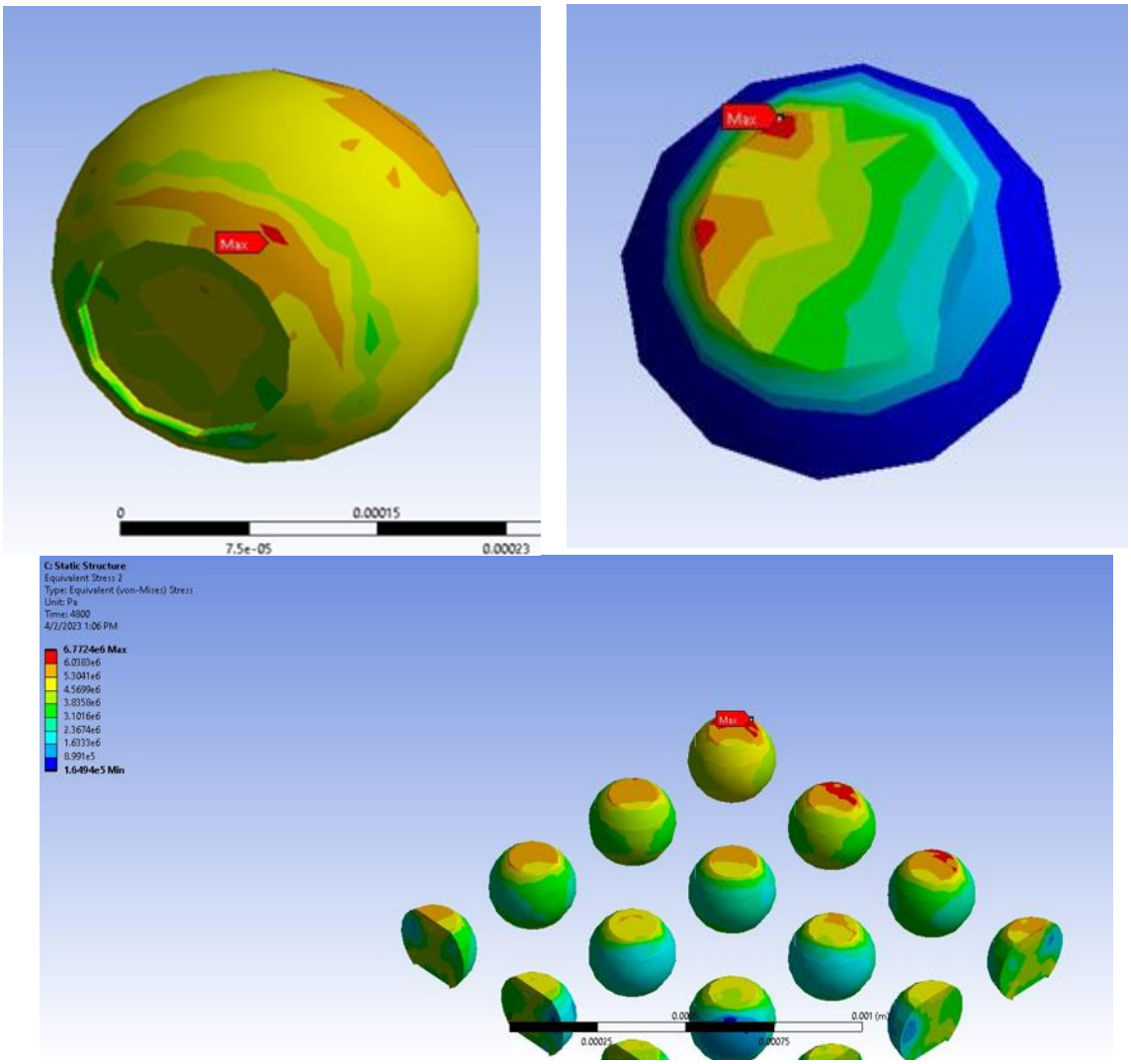

Fig. 11 Stress Distribution for 0.7mm

The calculation of plastic work using the developed APDL script has provided valuable insights into the mechanical behavior of two different printed circuit boards (PCBs) under investigation. Based on the stress and strain values obtained from the FEA model [28], the volume-average plastic work for the 1mm PCB was found to be 0.12 MPa, while the corresponding value for the 0.7mm PCB was 0.10 MPa. These results suggest that the 1mm PCB is more resistant to plastic deformation compared to the 0.7mm PCB, which may have important implications for their respective applications in industry.

4.1.1.1 Plastic Work (ΔW)

The calculation of volume-averaged plastic work is an essential step in determining the mechanical behavior of materials. [29]In this study, an ANSYS Parametric Design Language (APDL) script was developed to extract stress and strain data from the finite element analysis (FEA) model. [30]Using this script, the volume-averaged plastic work was determined for two different boards. The results of the analysis are presented below, providing insight into the plastic deformation behavior of the materials under investigation. [31]

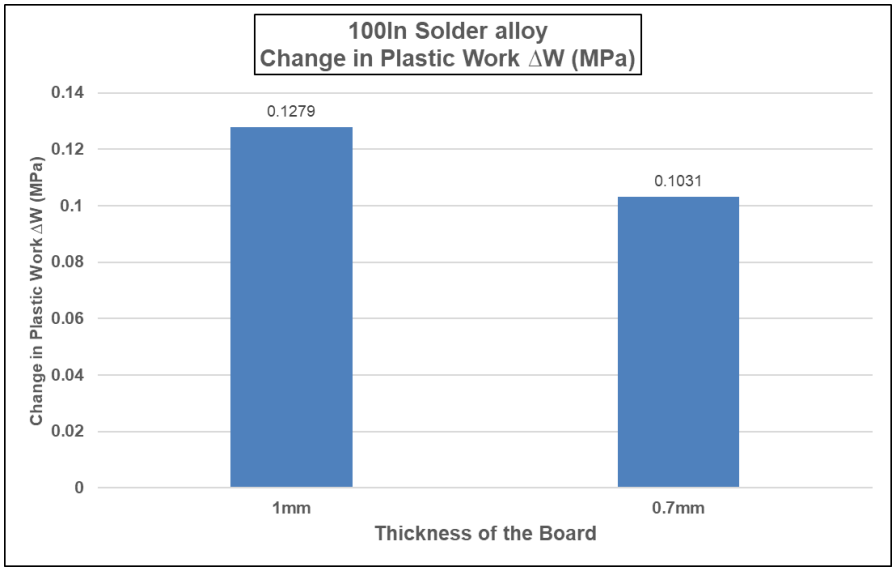

Fig. 12 Change in Plastic Work ΔW (MPa)

4.1.1.2 Number of Cycles to failure (N_f)

This volume-averaged plastic work is related to life cycles to failure using Schubert et al. and Che & Pang correlation [14]-

$$N_f=(A/\Delta W)\ ^k$$

Where Nf is the characteristic of life. A (in MPa) and k (unitless) are two empirical fatigue parameters that were used from Jie et al. work on chip-scale packages.

The values of A and k used were.

$$A = 8.783 \times 106 \text{ (MPa)},$$

$$k = 0.4701$$

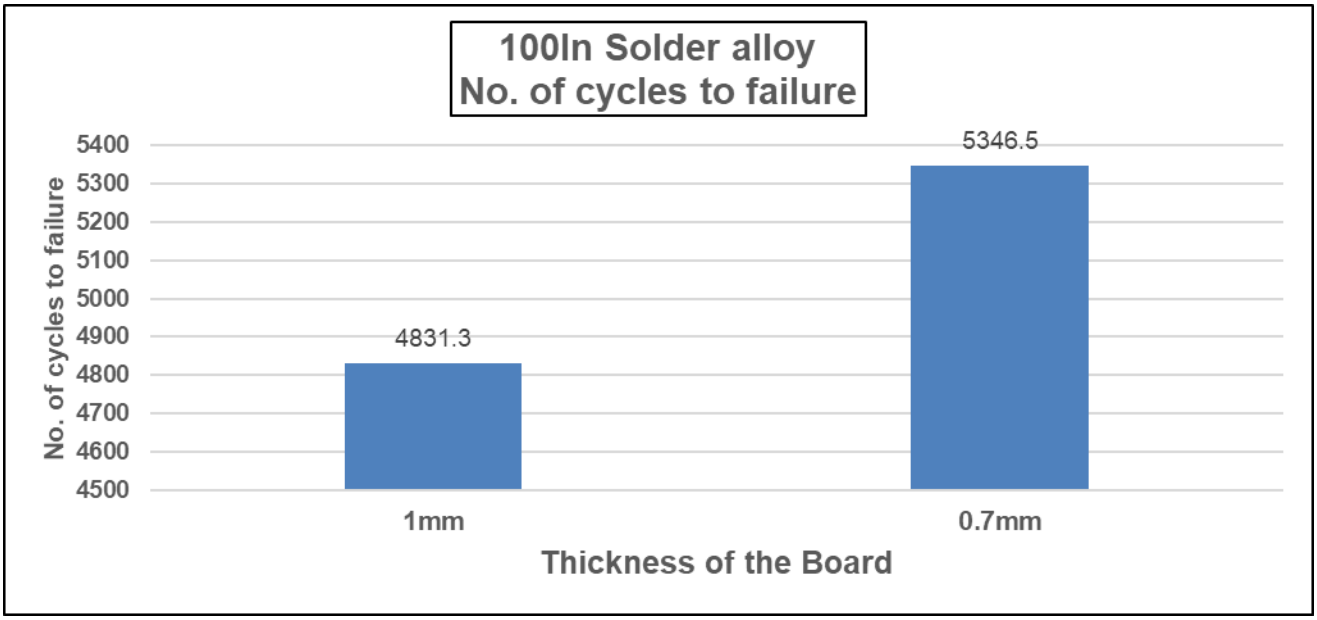

Fig. 13 No. of Cycles to failure

4.1.1.3 Conclusion

The calculated life cycles to failure (N_f) given in table below.

Board Thickness (mm)	Cycles to Failure (N_f)
1	4831
0.7	5346

Fig. 14 Life cycles to failure (N_f) - Comparison

As seen from the results above, the life cycles to failure in a 0.7mm board is 11% more than 1mm.

4.1.2 SAC 387 - 95.5%Sn - 3.8%Ag - 0.7%Cu

4.1.2.1 Stress Distribution

1mm PCB

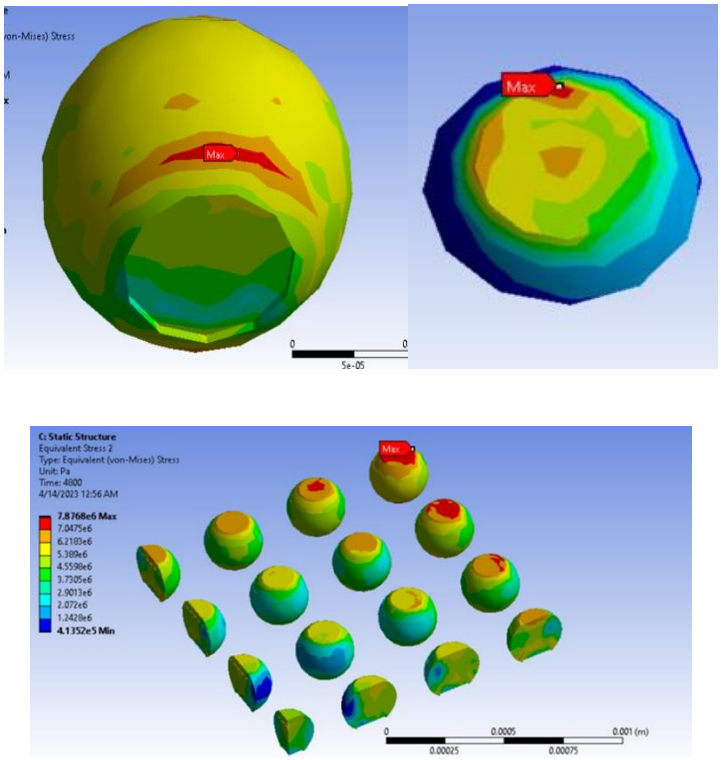

Fig. 15 Stress Distribution for 1mm

0.7mm PCB

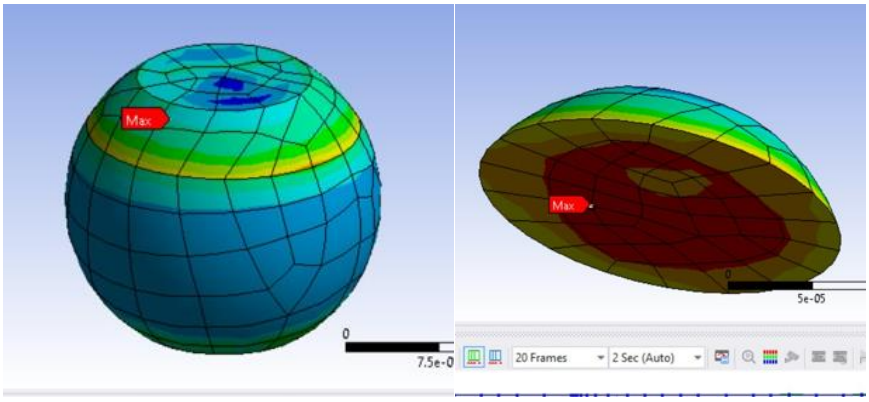

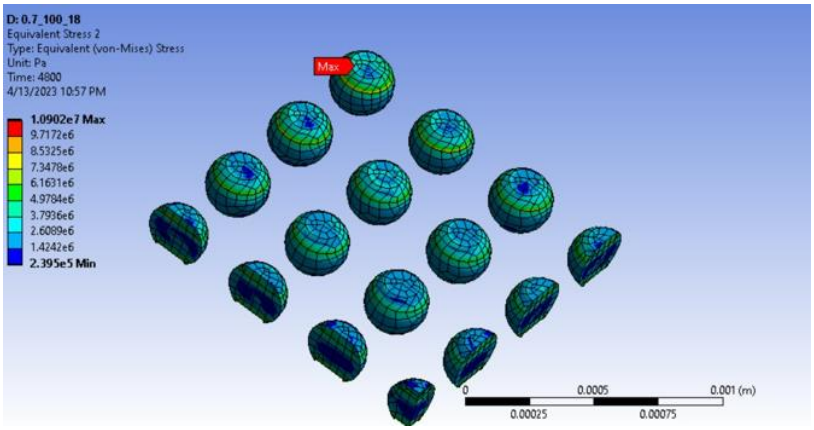

Fig. 16 Stress Distribution for 0.7mm

By conducting a detailed finite element analysis, the stress distribution was visualized, and a clear understanding of the areas of high stress concentration was gained. This information is crucial in determining the strength and durability of materials, as well as identifying potential areas of failure. [33]

4.1.2.2 Plastic Work (ΔW)

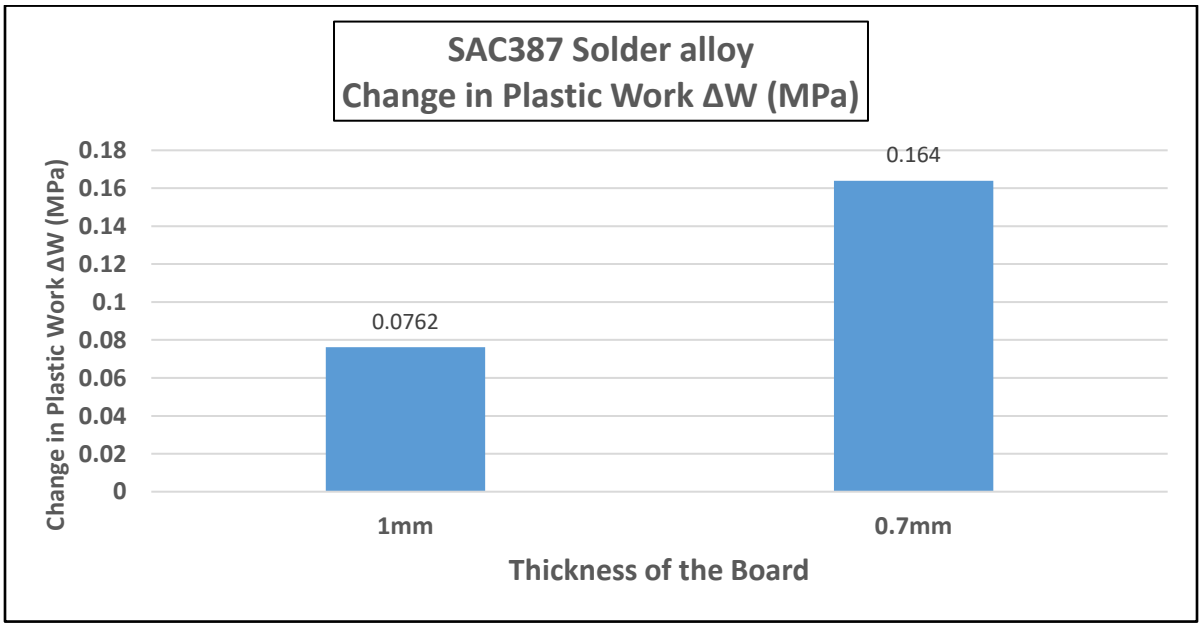

Fig. 17 Change in Plastic Work ΔW (MPa)

The calculation of volume-averaged plastic work is an essential step in determining the mechanical behavior of materials. In this study, an ANSYS Parametric Design Language (APDL) script was developed to extract stress and strain data from the finite element analysis (FEA) model. Using this script, the volume-averaged plastic work was determined for two different boards. The results of the analysis are presented below, providing insight into the plastic deformation behavior of the materials under investigation. [34]

4.1.2.3 Number of Cycles to failure (N_f)

This volume averaged plastic work is related to life cycles to failure using Schubert et al. and Che & Pang correlation- [35]

$$Nf=(A/\Delta W)\ ^k$$

Where N_f is the characteristic of life. A (in MPa) and k (unitless) are two empirical fatigue parameters that were used from Jie et al. work on chip-scale packages.

The values of A and k used were [36]

$$A = 8.783 \text{ x } 106 \text{ (MPa)},$$

$$k = 0.4701$$

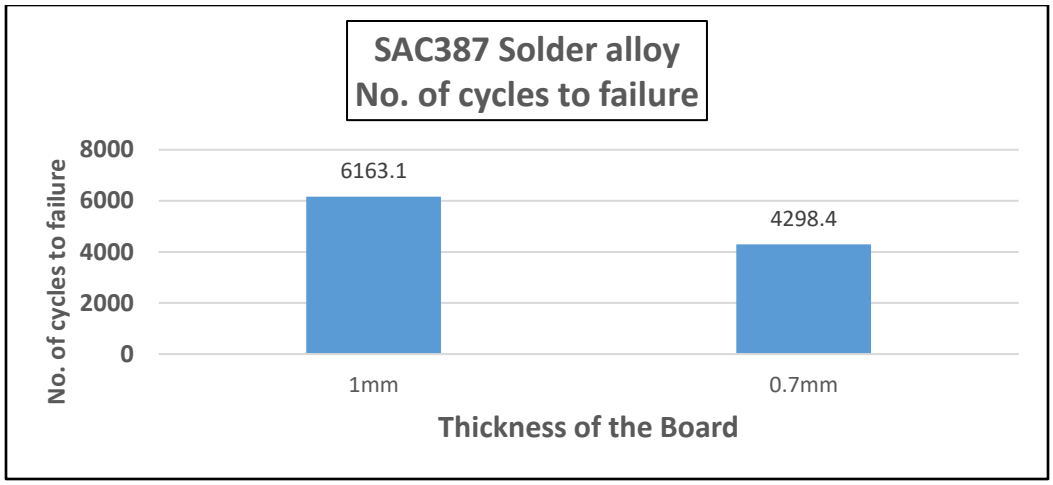

Fig. 18 No. of Cycles to failure

4.1.2.4 Conclusion

The calculated life cycles to failure (Nf) given in table below.

Board Thickness (mm)	Cycles to Failure (N_f)
1	6163
0.7	4298

Fig. 19 Life cycles to failure (N_f) - Comparison

As seen from the results above, the life cycles [37] to failure in a 1mm board is 36% more than 0.7mm.

4.1.3 SAC-Q - 92.7%Sn - 3.4%Ag - 0.5%Cu - 3.4%Bi

4.1.3.1 Stress Distribution

1mm PCB

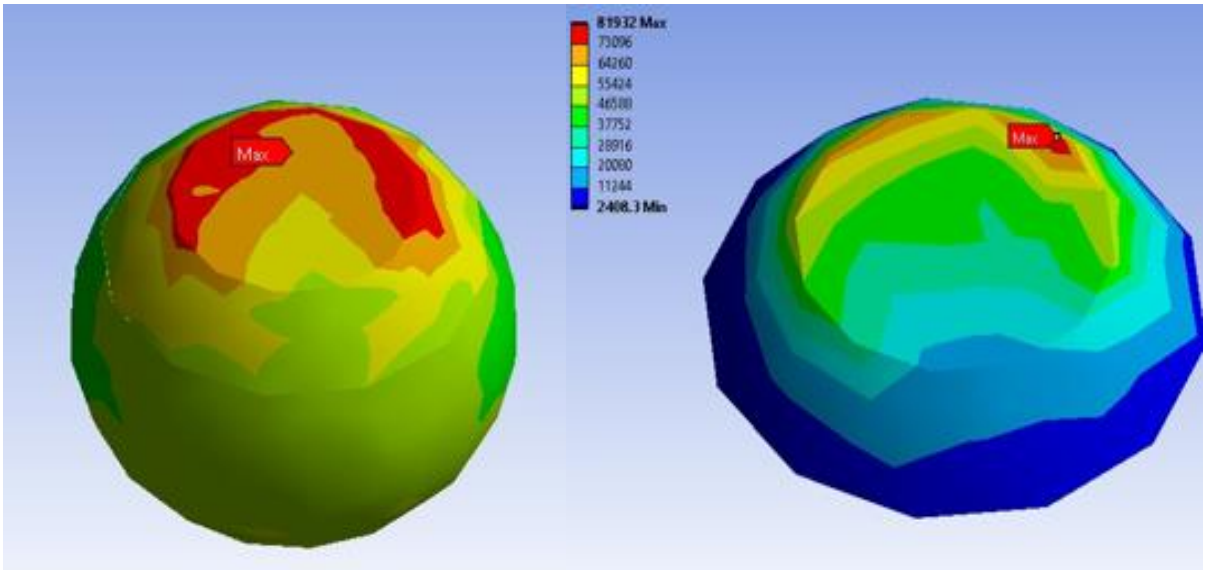

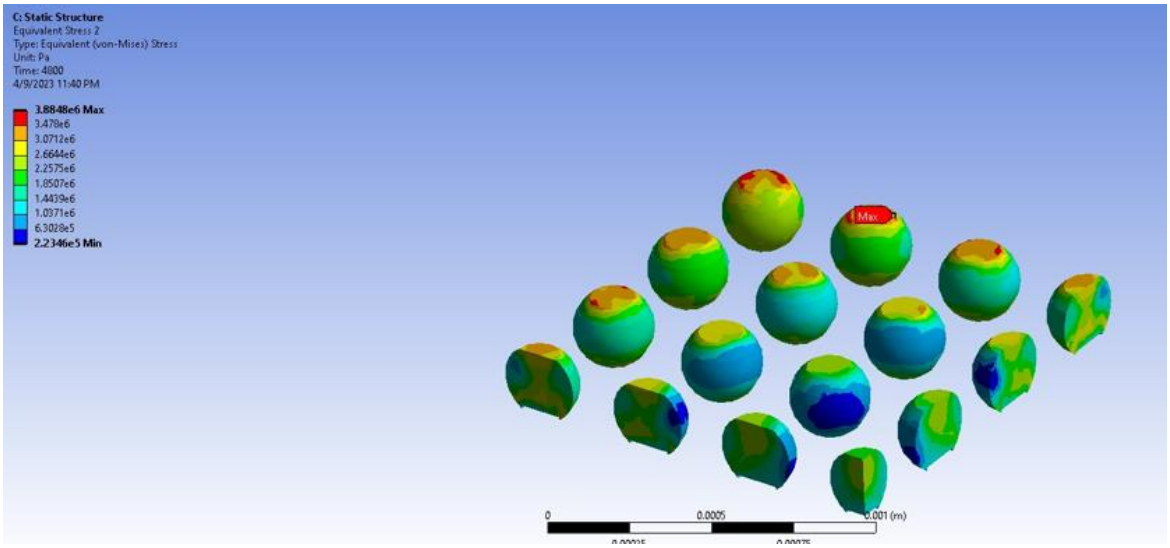

Fig. 20 Stress Distribution for 1mm

0.7mm PCB

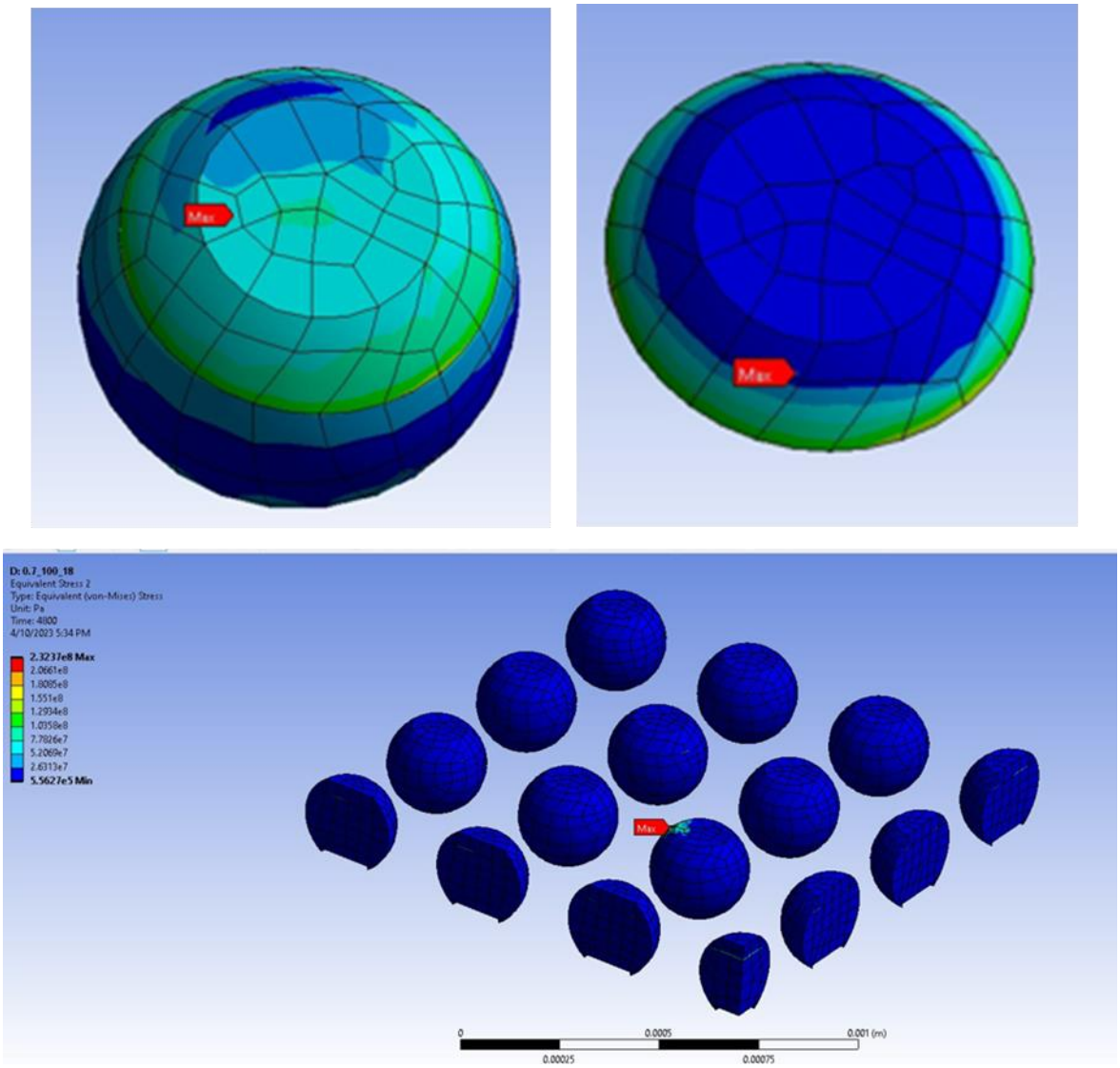

Fig. 21 Stress Distribution for 0.7mm

The use of bismuth in soldering is a common practice to improve the wetting properties of the material and reduce surface tension. In this study, the addition of bismuth was investigated to determine its effects on the stress distribution during the soldering process. The results of the analysis revealed that the stress distribution was concentrated on the corner regions, irrespective of the presence of bismuth in the solder material. [38]

4.1.3.2 Plastic Work (ΔW)

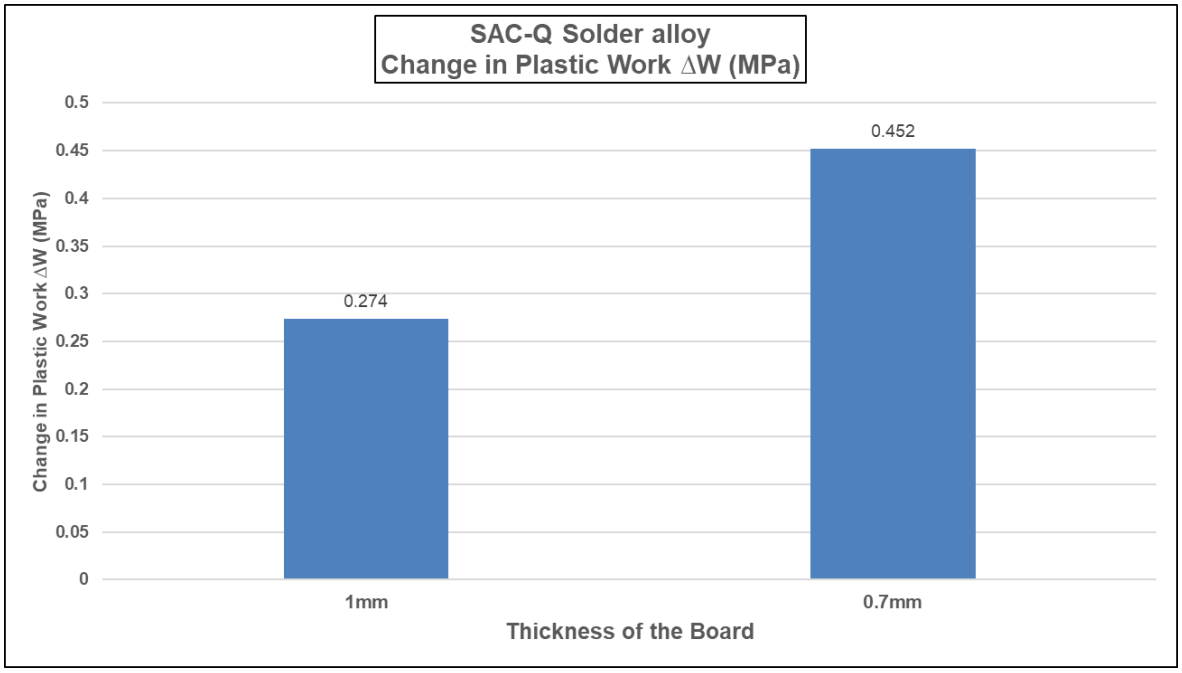

Fig. 21 - 1 Change in Plastic Work ΔW (MPa)

The analysis of the plastic work for the two different board thicknesses revealed interesting findings. The 1mm board exhibited a plastic work value of 0.27 MPa, whereas the 0.7mm board had a plastic work value of 0.45 MPa. These results indicate that the 0.7mm board underwent a higher level of plastic deformation compared to the 1mm board. This observation may be attributed to the fact that the thinner board experienced a greater level of stress concentration, leading to increased plastic deformation. These findings are valuable in understanding the mechanical properties of the materials and can be used to optimize the design and performance of similar components.

4.1.3.3 Number of Cycles to failure (N_f)

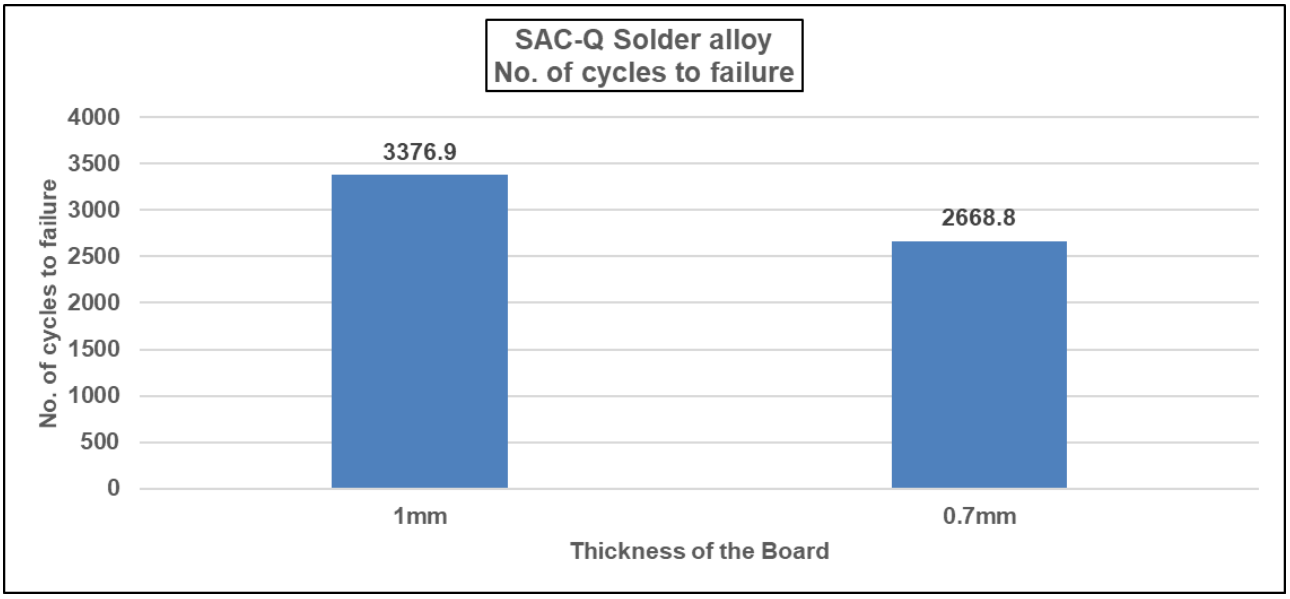

Fig. 22 No. of Cycles to failure

In this study, the 1MM board was subjected to cyclic loading, and the number of cycles to failure was determined. The results show that the board with a thickness of 1MM lasted for 3376 cycles before failure occurred. Moreover, the impact of the stress ratio was also evaluated, and the board's endurance was found to be reduced when the stress ratio was increased to 0.7, with a failure occurring at 2668 cycles.

4.1.3.4 Conclusion

Board Thickness (mm)	Cycles to Failure (N_f)
1	3376
0.7	2668

Fig. 23 Life cycles to failure (N_f) – Comparison

In this study, two different boards were subjected to fatigue testing, and their lifecycle to failure was calculated. The results showed that the thicker board exhibited a 24% increase in lifecycle to failure compared to the 0.7mm board. [39]This indicates that the thicker board possesses superior fatigue resistance and can withstand more cycles of loading before failure.

Chapter 5 Evaluation - Overall

5.1 Stress Distribution

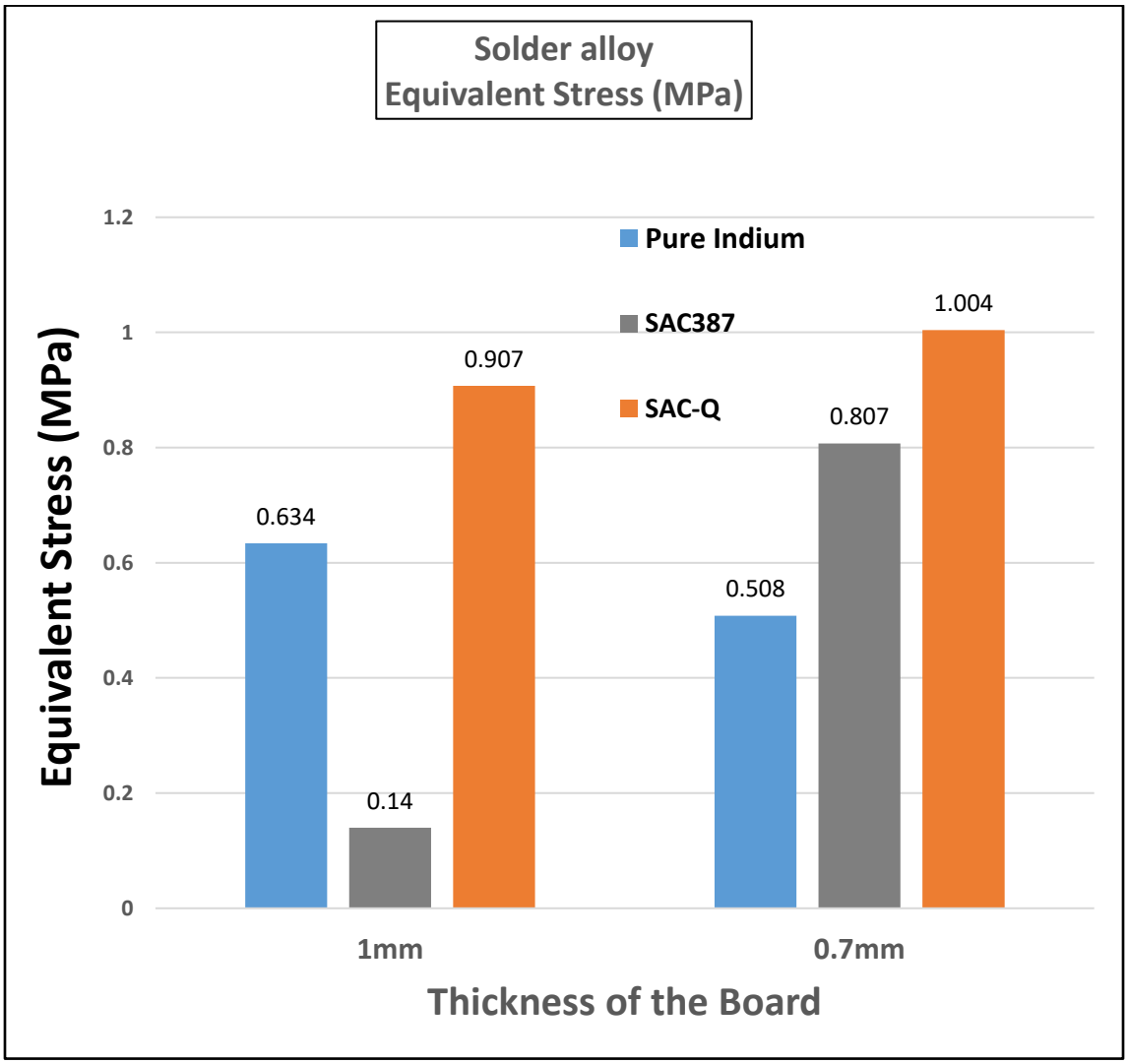

Fig. 24 Stress Distribution – Comparison

5.1.1 Plastic Work (ΔW)

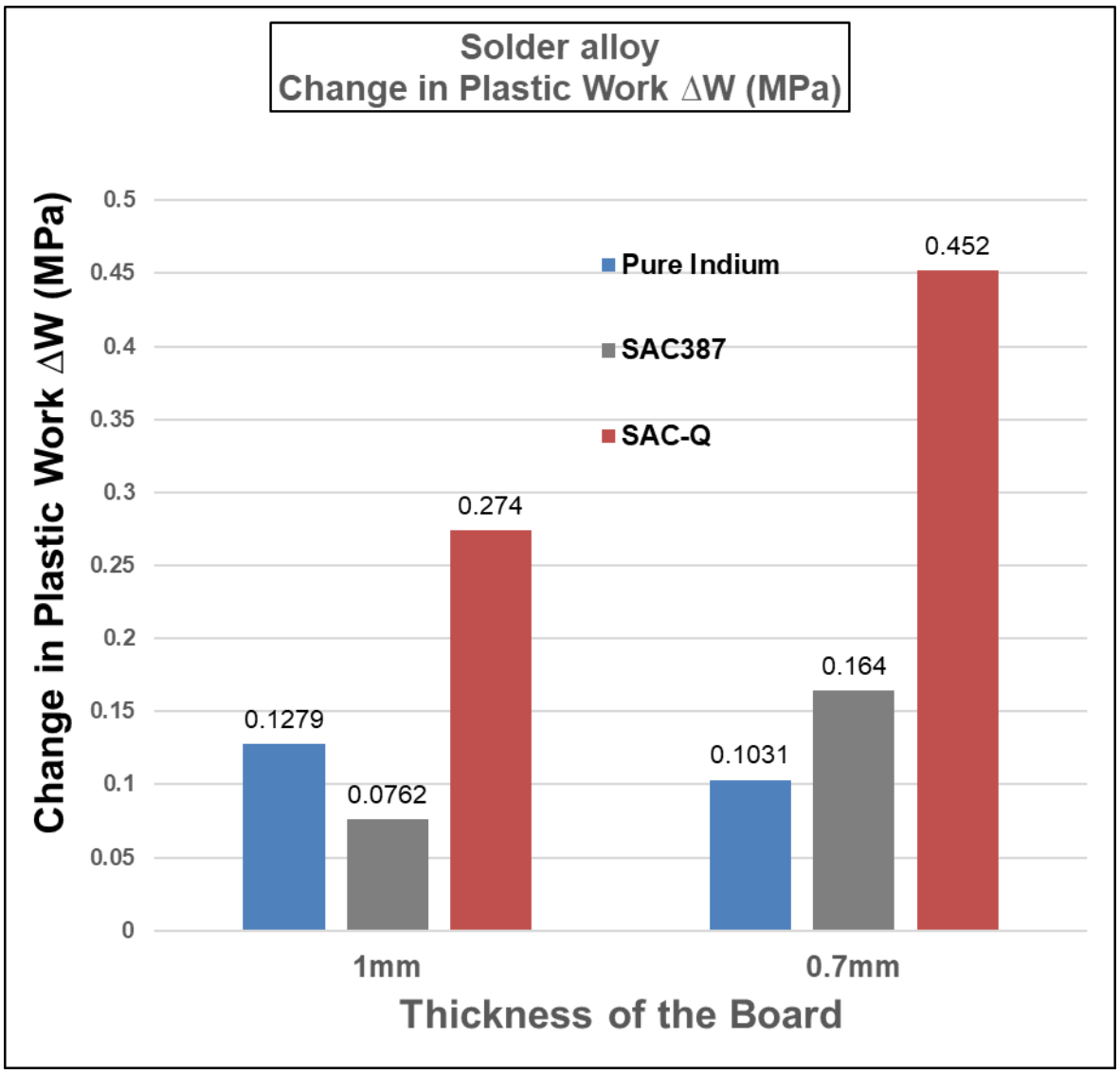

Fig. 25 Plastic Work (ΔW)– Comparison

5.1.2 Number of Cycles to failure (N_f)

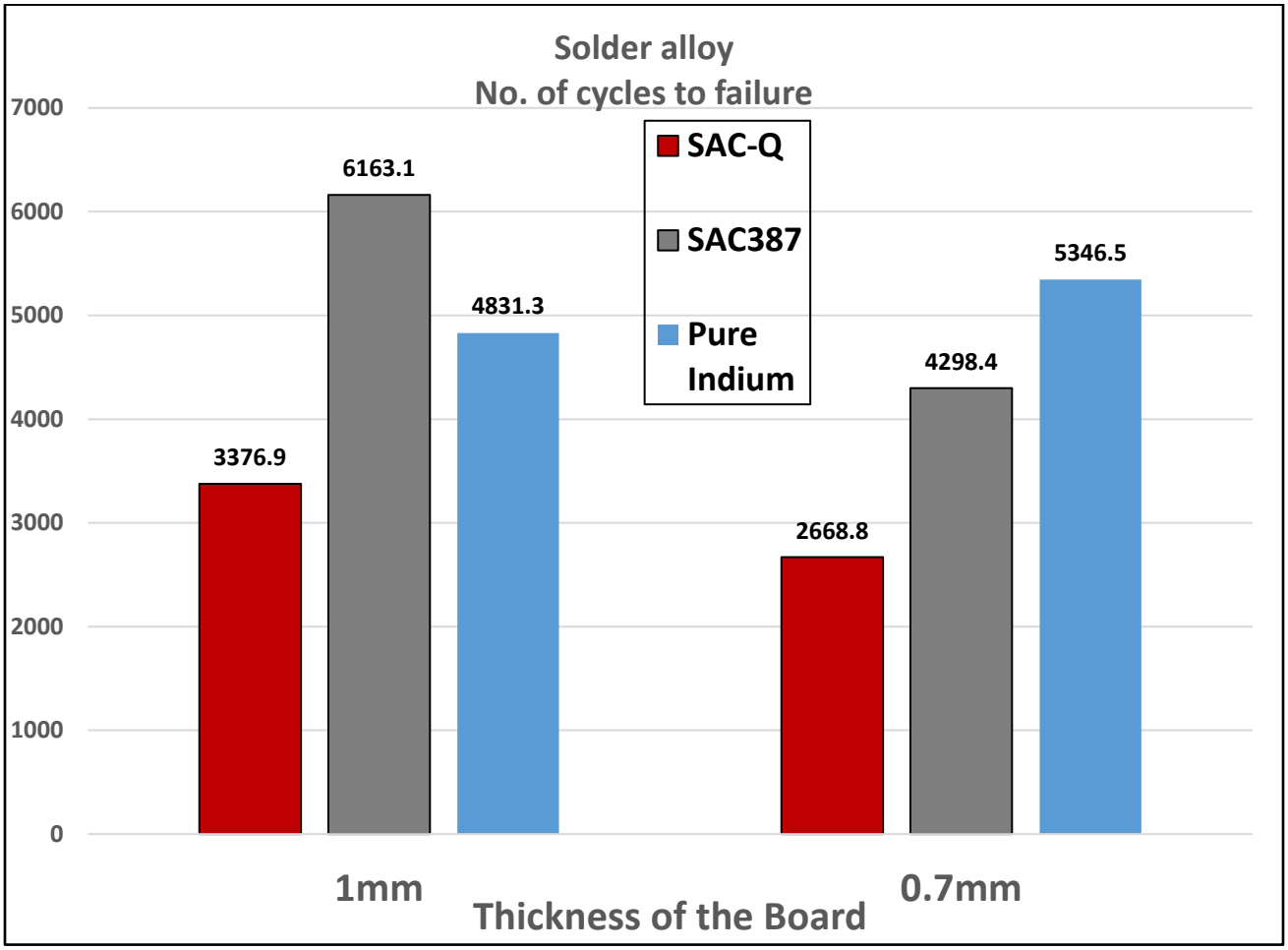

Fig. 26 No. of Cycles to failure

Chapter 6 Parametric Study

6.1 Design of Experiments - Data and Comparison

Component	CTE (ppm/°C)	E (GPa)
PCB (1mm)	15	25
PCB (0.7mm)	18	30

Fig. 27 Baseline PCB

1mm PCB

Solder Alloys	Pure Indium	SAC387	SAC-Q
% Increase (No of cycles to failure)	15%	30%	23%

Fig. 28 DP1 Results for 1mm

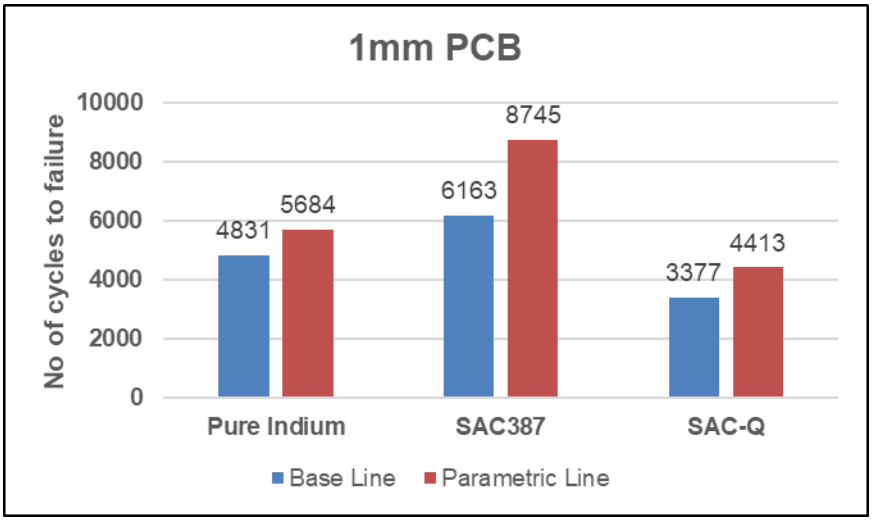

Fig. 29 Baseline vs Parametric for 1mm

0.7mm PCB

Solder Alloys	Pure Indium	SAC387	SAC-Q
% Increase (No of cycles to failure)	20%	19%	29%

Fig. 30 DP1 Results for 0.7mm

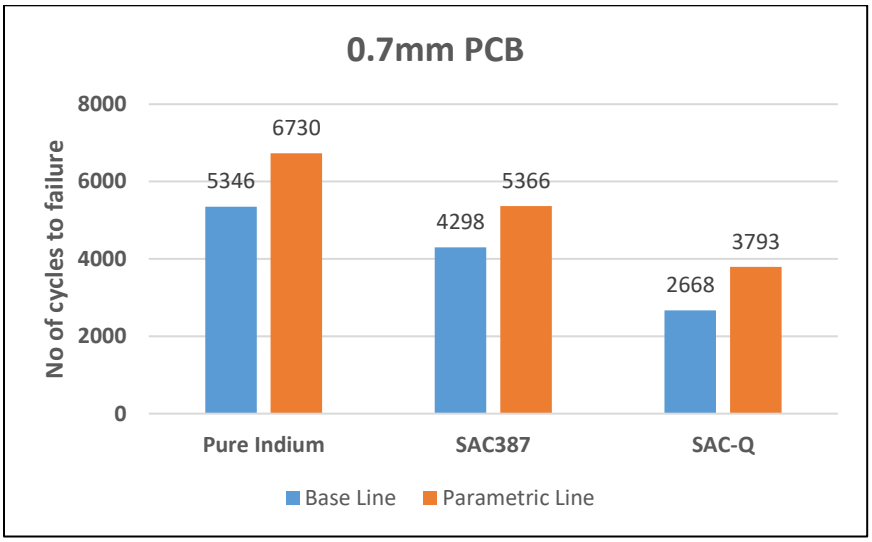

Fig. 31 Baseline vs Parametric for 0.7mm

Design of Experiments

Design Points	CTE (ppm/°C)	E (GPa)
DP1	05	15
DP2	08	20
DP3	15	25
DP4	18	30
DP5	25	35
DP6	35	40

Fig. 32 Design of Experiments

Chapter 7 Conclusion

In conclusion, the FEA analysis conducted in this study demonstrated that the choice of solder material and PCB thickness has a significant impact on the reliability of solder joints. [40]For the 1mm PCB, SAC 387 solder exhibited the highest number of cycles to failure, while for the 0.7mm PCB, Pure Indium solder showed the highest number of cycles to failure. These results highlight the importance of carefully selecting the solder material and PCB thickness based on the specific application requirements to ensure optimal reliability. [41]

Furthermore, [42] the parametric study revealed that Young's modulus of a PCB plays a critical role in determining its sensitivity to solder joint reliability issues. [43]A lower coefficient of thermal expansion (CTE) or proximity to the silicon die was found to result in less plastic work and ultimately, more cycles to failure. [44]Overall, these findings emphasize the need for a comprehensive understanding of the mechanical behavior of PCBs and solder materials to optimize reliability and performance in electronic devices.

References

[1] H. v. H. (. W. B. (. Jan Eite Bullema (TNO), "Guidelines for Packaging of Microfluidics: Electrical Interconnections".

[2] R. B. D. A. Abel Misrak, "Viscoelastic Influence on the Board Level Assessment of Wafer Level Packages Under Drop Impact and Under Thermal Cycling," *ASME,* 2023.

[3] M. M. R. 1. 2. M. K. 1. P. P. D. 1. 2. R. B. 1. R. R. 1. 2. D. A. 1. A S M Raufur Chowdhury 1, "A Comparative Study of Thermal Aging Effect on the Properties of Silicone-Based and Silicone-Free Thermal Gap Filler Materials," *National Library of Medicine,* 2021.

[4] T. Chauhan, R. Bhandari, A. S. M. R. Chowdhury, A. Lakshminarayana, F. Mirza, B. G. Bazehhour, M. Vujosevic and D. Agonafer, "Impact of Die Attach Sample Preparation on Its Measured Mechanical Properties for MEMS Sensor Applications," *Journal of Microelectronics and Electronic Packaging,* 2021.

[5] R. Shashikanth, "https://www.protoexpress.com/blog/bga-features-soldering-x-ray-inspection/," [Online]. Available: https://www.protoexpress.com/blog/bga-features-soldering-x-ray-inspection/.

[6] "Tin Solder, Lead Solder, Flux-core Solder, and Rosin-core Solder– Differences and Uses," [Online]. Available: https://components101.com/article/different-types-of-solders-tin-solder-lead-solder-flux-core-solder-and-rosin-core-solder.

[7] I. K. O. Krammer, "Method for selective solder paste application for BGA rework," 2008.

[8] P. RAJMANE, "MULTI-PHYSICS DESIGN OPTIMIZATION OF 2D AND ADVANCED HETEROGENOUS 3D INTEGRATED CIRCUITS," 2018.

[9] A. B. LAKSHMINARAYANA, "IMPACT OF VISCOELASTIC PROPERTIES OF LOW LOSS PRINTED," 2020.

[10] Z. Z. b. Tong Yan Tee a, "Board level solder joint reliability analysis and optimization of pyramidal stacked die BGA packages," *Science Direct,* 2004.

[11] ∗. R. B. Tushar Chauhan, "IMPACT OF IMMERSION COOLING," *Journal of Enhanced Heat Transfer,* 2021.

[12] B. CONJEEVARAM, "SOLDER BALL RELIABILITY ASSESSMENT OF WAFER LEVEL CHIP SCALE PACKAGE (WLCSP) THROUGH POWER CYCLING," 2016.

[13] T. SHETTY, "BOARD LEVEL RELIABILITY ASSESMENT OF THICK FR-4 QFN ASSEMBLIES UNDER THERMAL CYCLING," 2014.

[14] F. X. Che and J. H. L. Pang, "Fatigue Reliability Analysis of Sn–Ag–Cu Solder Joints Subject to Thermal Cycling," *IEEE Xplore,* 2012.

[15] M. A. Silaghi, Dielectric Material, Rijeka, Croatia: InTech, 2012.

[16] C. J. Lasance, C. T. Murray, D. L. Saums and M. Rencz, "Challenges in Thermal Interface Material Testing," in *Twenty-Second Annual IEEE Semiconductor Thermal Measurement And Management Symposium*, Dallas, TX, USA, 2006.

[17] D. D. L. Chung , "Thermal interface materials," *Journal of Materials Engineering and Performance volume 10(1),* pp. 56-59, 2001.

[18] J. H. Lau, Heterogeneous Integrations, Springer, Singapore, 2019.

[19] R. Skuriat, J. F. Li, P. A. Agyakwa, N. Mattey, P. Evans and C. M. Johnson, "Degradation of thermal interface materials for high-temperature power electronics applications," *Microelectronics Reliability,* vol. 53, no. 12, pp. 1933-1942, 2013.

[20] Taylor & Francis Group, Physical Design for 3D Integrated Circuits, A. Todori-Sanial and C. S. Tan, Eds., Boca Raton, FL: Taylor & Francis Group, LLC, 2016.

[21] U. Rahangdale, "STRUCTURAL OPTIMIZATION & RELIABILITY OF 3D PACKAGE BY STUDYING CRACK BEHAVIOR ON TSV & BEOL & IMPACT OF POWER CYCLING ON RELIABILITY FLIP CHIP PACKAGE," Arlington, TX, 2017.

[22] B. Rodgers, J. Punch, J. Jarvis, P. Myllykoski and T. Reinikainen, "FINITE ELEMENT MODELLING OF A BGA PACKAGE SUBJECTED TO THERMAL AND POWER CYCLING," in *Inter Society Conference on Thermal Phenomena*, San Diego, CA, USA, 2002.

[23] Pavan Rajmane, F. Mirza, H. Khan and D. Agonafer, "Chip Package Interaction Study to Analyze the Mechanical Integrity of a 3-D TSV Package," in *ASME 2015 International Technical Conference and Exhibition on Packaging and Integration of Electronic and Photonic Microsystems collocated with the ASME 2015 13th International Conference on Nanochannels, Microchannels, and Minichannels*, 2015.

[24] C. K. Roy, S. Bhavnani, M. . C. Hamilton, R. Johnson, R. W. Knight and D. K. Harris, "Accelerated aging and thermal cycling of low melting temperature alloys as wet thermal interface materials," *Microelectronics Reliability*, vol. 55, no. 12, pp. 2698-2704, December 2015.

[25] B. . A. Cola, "Carbon nanotubes as high performance thermal interface materials," *Electronics Cooling,* vol. 16, pp. 10-15, Spring 2010.

[26] J. R. Wasniewski, D. H. Altman, S. L. Hodson, T. S. Fisher, A. Bulusu, S. Graham and B. A. Cola, "Characterization of Metallically Bonded Carbon Nanotube-Based Thermal Interface Materials Using a High Accuracy 1D Steady-State Technique," *ASME Journal of Electronic Packaging,* June 2012.

[27] J. P. Gwinn and R. L. Webb, "Performance and testing of thermal interface materials," *Microelectronics Journal,* vol. 34, no. 3, p. 215–222, March 2003.

[28] K. P. PRAMODA and T. LIU, "Effect of Moisture on the Dynamic Mechanical Relaxation of Polyamide-6/Clay Nanocomposites," *Journal of Polymer Science Part B: Polymer Physics*, vol. 42, no. 10, pp. 1823-1830, May 2004.

[29] "International Technology Roadmap for Semiconductors 2.0, 2015 Edition, Heterogenous Integration," 2015.

[30] A. Todri-Sanial and C. S. Tan, Physical Design for 3D Integrated Circuits, Boca Raton, FL: Taylor & Francis Group, LLC, 2016.

[31] P. Rajmane, "Multi-Physics Design Optimization of 2D and Advanced Heterogenous 3D Integrated Circuit," Arlington, TX, 2018.

[32] Environmental & Vibration Testing Equipment Manufacturer, "SE-600-10-10 Environmental Chamber," Environmental & Vibration Testing Equipment Manufacturer, [Online]. Available: https://thermotron.com/equipment/se-series-detail/se-600-10-10-environmental-chamber/. [Accessed 30 April 2020].

[33] Cadence, "3D ICs with TSVs—Design Challenges and Requirements," 2018.

[34] JEDEC Solid State Technology Association, "High Temperature Storage Life," JEDEC, 2015.

[35] KITAGAWA Industries America, Inc., "Silicone-Free Thermal Pad," KITAGAWA Industries America, Inc., [Online]. Available: http://kgs-ind.com/products/thermal-pads/silicone-free-thermal-pads/. [Accessed 01 May 2020].

[36] Sun Electronic Systems, Inc., "MODEL EC127, TEMPERATURE TEST CHAMBER USER MANUAL," Sun Electronic Systems, Inc., 1995.

[37] Hitachi High-Tech Corporation, "Principle of Dynamic Mechanical Analysis (DMA)," Hitachi High-Tech Corporation, [Online]. Available: https://www.hitachi-hightech.com/global/products/science/tech/ana/thermal/descriptions/dma.html. [Accessed 02 May 2020].

[38] Hitachi High-Tech Corporation, "Principle of Thermomechanical Analysis (TMA)," [Online]. Available: https://www.hitachi-hightech.com/global/products/science/tech/ana/thermal/descriptions/tma.html. [Accessed 02 May 2020].

[39] A. Misrak, T. Chauhan, P. Rajmane, R. Bhandari and D. Agonafer, "Impact of Aging on Mechanical Properties of Thermally Conductive Gap Fillers," *ASME Journal of Electronic Packaging*, vol. 142, no. 1, March 2020.

[40] Hitachi High-Tech Science Corporation, "Operational Manual, 0503-513-001E Ver.2.0, TA7000 Series, Dynamic Mechanical Analyzer," Hitachi High-Tech Science Corporation, 2013.

[41] EDEC Solid State Technology Association, "Highly Accelerated Temperature and Humidity Stress Test (HAST), JESD22-A110E," JEDEC, 2015.

[42] J. Due and A. J. Robinson, "Reliability of thermal interface materials: A review," *Applied Thermal Engineering*, vol. 50, no. 1, pp. 455 - 463, 2013.

[43] D. Chung, "Materials for thermal conduction," *Applied Thermal Engineering*, vol. 21, no. 16, pp. 1593-1605, 2001.

[44] N. Goel, T. K. Anoop, A. Bhattacharya, J. A. Cervantes, R. K. Mongia, S. V. Machiroutu, H.-L. Lin, Y.-C. Huang, K.-C. Fan, B.-L. Denq, C.-H. Liu, C.-H. Lin, C.-W. Tien and J.-H. Pan, "TECHNICAL REVIEW OF CHARACTERIZATION METHODS FOR THERMAL INTERFACE MATERIALS (TIM)," in *11th Intersociety Conference on Thermal and Thermomechanical Phenomena in Electronic Systems*, Orlando, FL, USA, 2008.